buildings

MDPI

Review

Structural Vibration Comfort: A Review of Recent Developments

Weiping Xie and Yumeng Hua *

School of Civil Engineering and Architecture, Wuhan University of Technology, Wuhan 430070, China; xiewp@whut.edu.cn

* Correspondence: huaym@whut.edu.cn

Abstract: With continuous improvements in the social economy and living standards of individuals, the vibration comfort of building structures has gradually been emphasized by academic and engineering communities, such as vehicle-induced vibrations in buildings near traffic, human-induced vibrations in large-span structures, wind-induced vibrations in super-high-rise buildings, and machinery-induced structural vibrations. Comfort-based structural analysis is distinct from traditional safety-based structural analysis, and its theoretical systems and unified guidelines have not yet been established. This paper reviews recent research on structural vibration comfort, including major load categories and their impacts, comfort-based structural analysis, evaluation methods, and vibration-mitigation measures. By presenting the shortcomings of the existing research, potential topics for future study are suggested.

Keywords: vibration comfort; serviceability; environmental vibration; vehicle-induced vibration; human-induced vibration; wind-induced vibration; machinery-induced vibration; structural analysis; comfort evaluation; vibration control

Citation: Xie, W.; Hua, Y. Structural Vibration Comfort: A Review of Recent Developments. *Buildings* **2024**, *14*, 1592. https://doi.org/10.3390/buildings14061592

Academic Editors: Fabrizio Gara, Haoran Zuo, Kunjie Rong, Ruisheng Ma and Siyuan Wu

Received: 29 March 2024
Revised: 18 May 2024
Accepted: 23 May 2024
Published: 31 May 2024

1. Introduction

With the upgrading of construction technology, application of lightweight and high-strength materials, realization of new structural systems, and pursuit of architectural aesthetics, modern engineering structures tend to develop in light, flexible, large-span, and towering designs. This change has resulted in an apparent decrease in the structural self-vibration frequency, which is close to the frequency of traffic vehicles, wind, dynamic machinery, and people's daily activities; thus, it is prone to resonance and generates a significant dynamic response. Such structural vibration is generally not sufficient to cause safety problems, but it can cause uncomfortable feelings for the people in the building, which is a comfort problem. People in such vibrating environments can appear nervous, annoyed, or panicky, which may result in mental illness over time. Therefore, in the design and construction of "sensitive buildings" (e.g., buildings near traffic, large-span structures, super-high-rise structures, and buildings with dynamic machinery inside), the structural dynamic response is predicted or measured, and vibration control measures are applied if the response levels exceed comfort standards. Such engineering cases have increased in number in recent years.

Research on vibration comfort began in 1931, when Reiher and Meier conducted pioneering experiments, developed preliminary conclusions on how vibration frequency affects human comfort, and provided a paradigm for comfort studies [1]. Subsequently, scholars in the United States, Europe, and Japan have conducted numerous studies and issued a series of specifications and guidelines [2–7]. Griffin's team conducted a representative study, investigating the effects of frequency, direction, and duration of vibration, human posture, and other factors of the human vibration perception threshold through a number of experiments [5]. The Millennium Bridge vibration event in London, UK, in 2000 brought widespread attention to the comfort of pedestrian bridge structures

by scholars and engineers [8,9], subsequently drove the study of structural comfort caused by human-induced loads, and provided a strong impetus to research in this field. Researchers have accumulated numerous results on structural vibration comfort.

High-speed railways and urban rail transits that have developed rapidly in China since the 1980s facilitate resident travel, but also induce environmental vibrations that have caused complaints from nearby residents [10,11]. With improvements in quality of life, people's demand for living environments has also increased. Environmental vibration is defined as an environmental ground motion of small amplitude resulting from natural and/or anthropogenic causes (traffic, human-induced excitation, wind, and machinery excitation) [12]. To address this problem, Chinese scholars have focused attention on research into vibration comfort.

In addition to comfort problems, environmental vibrations cause negative impacts, including secondary noise, failure of precision instruments, damage to non-structural components, safety of ancient buildings, and wildlife preservation. Most of these issues do not involve structural safety and primarily affect architectural functions or structural serviceability. In engineering, these non-safety issues are sometimes all included in comfort analyses, but some of the above analyses do not conform to the definition of comfort. Environmental vibrations are the cause of comfort problems; however, comfort problems are not the only hazards caused by environmental vibrations. In the literature regarding structural vibration comfort, the term "serviceability" is used, but it differs from the connotation of comfort. In the International Organisation for Standardisation (ISO) publication ISO 5805-1997 Mechanical vibration and shock—Human exposure—Vocabulary [13], "comfort" is defined as the subjective state of well-being or absence of mechanical disturbance in relation to the induced environment (mechanical vibration or repetitive shock). This indicates that "comfort" is the subjective feeling of vibration by the user in the structure. "Serviceability" has a broad scope. The ISO publication ISO 10137: 2007 Bases for design of structures—Serviceability of buildings and walkways against vibrations [14] describes the receivers in vibration serviceability problems, which can encompass the building structure (or components such as beams, slabs, walls, and windows, among others), contents of the building (instrument and machinery among others), or human occupants of the building. It indicates that "serviceability" includes not only human comfort but also vibration-induced damage to structures or components (e.g., safety of ancient buildings, non-structural component cracking) and the regular operation of precision instruments.

This paper reviews the progress of research on structural vibration comfort. Section 2 systematically illustrates the comfort problems induced by loads of traffic vehicles, humans, wind, and dynamic machinery. Section 3 discusses comfort-based structural analysis methods and describes the key modeling and calculation details. Section 4 summarizes the comfort evaluation methods. Section 5 illustrates the existing vibration mitigation measures employed in vibration comfort control. Section 6 suggests potential topics and directions for study in light of the shortcomings of current research.

2. Load Categories and Impacts on Vibration Comfort

Statistics in China in 2020 indicate that the sources that induce vibration comfort problems include traffic (26.4%), humans (34.5%), wind (19.1%), dynamic machinery (12.7% commonly and 5.8% for construction), and others (1.5%) [15]. Load categories differ in terms of source characteristics, action position, corresponding sensitive structure type, and dynamic response law. This section surveys the vibration comfort problems induced by each of the four load categories.

2.1. Vehicle-Induced Vibration

Vehicle-induced vibration is the dynamic response of structures caused by the movement of trains, such as high-speed, subway, and maglev trains, or motor vehicles, such as cars, buses, and heavy-duty trucks. In this subsection, research on the vehicle load model,

vibration propagation in soil and soil–structure interaction (SSI), and a simplified calculation approach are presented.

2.1.1. Vehicle Load Model

Research on vehicle-load models began with theoretical and experimental studies of vehicles crossing bridges by Willis and Stokes in 1849 [16,17]. The initial classical theoretical methods simplified the vehicle as a moving constant force, moving harmonic force, moving mass, or moving sprung mass and used analytical methods to obtain dynamic responses, as shown in Figure 1a–d. In the moving mass model illustrated in Figure 1c, the force applied on the ground is represented by Equation (1), considering the lateral inertial of the moving object. By disregarding the lateral inertia, Equation (1) simplifies to Equation (2), transforming the model into the moving load shown in Figure 1a [18,19].

$$F(x,t) = M\left(g - \frac{\mathrm{d}^2 w}{\mathrm{d}t^2}\right)\delta(x - x_M) \tag{1}$$

$$F(x,t) = Mg\delta(x - x_M) \tag{2}$$

where g is the gravitational acceleration; $w = w(x,t)$ denotes the lateral deformation of the underlying structure; δ denotes the Dirac delta function; x_M represents the longitudinal coordinate of the moving mass on the ground.

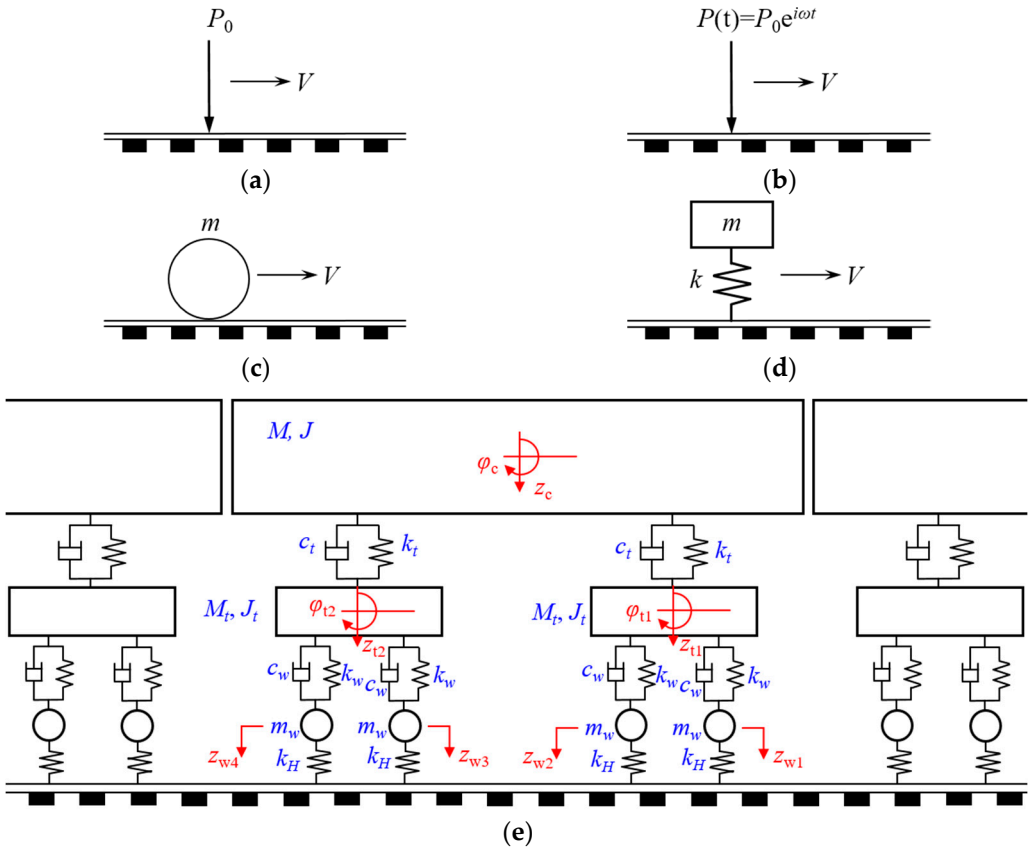

Figure 1. Vehicle load models: (**a**) moving constant force; (**b**) moving harmonic force; (**c**) moving mass; (**d**) moving sprung mass; (**e**) 10-DOF multi-rigid-body model (DOFs are marked in red; mass, stiffness, and damping coefficients are marked in blue).

Since the 1970s, with the development of computer and numerical techniques, vehicle models based on multi-rigid-body dynamics have gradually become the mainstream methods. Chu et al. [20] initially simplified the railway vehicle as a three-degree-of-freedom model system consisting of the car body and wheel–axle sets, after which the degree

of freedom (DOF) of developed vehicle models was continuously increased. Figure 1e shows a plane 10-DOF train model popularly used in the prediction of vehicle-induced environmental vibration [10]. This method considers the train–track (or car–road) coupling effect, sets the wheel–rail (or road) contact relationship, uses track irregularity (or road surface roughness) as the main source of excitation, and calculates the equations of motion using iterative or energy methods. Over the years, this vehicle modeling method and its computational theories have tended to be complete and are now applicable to various vehicle types, such as trains and cars, and many related monographs have been published [10,21,22].

Research in this field has mainly been conducted by researchers in the disciplines of vehicle, railway, and bridge engineering. Their primary objective in developing vehicle load models and dynamic analyses was to determine passenger comfort or the safety and durability of train running, railways, or bridges. Table 1 lists the typical train load models in recent years. Therefore, their vehicle load models are sufficiently detailed, with the latest model having 42 DOFs [23]. However, when the purpose of dynamic analysis is turned to the comfort of building structures, theoretically, a vehicle model with fewer DOFs and simplified track and wheel–rail contact relationships can satisfy the accuracy requirement for comfort analyses because of the filtering properties of soil for high-frequency vibrations and the low-frequency characteristics of structures. In the existing literature on comfort analysis, the train models used for calculations include several types of multi-rigid-body models, such as plane models (e.g., 10 DOFs [10,24]) and space models (e.g., 35 DOFs [25,26]). Furthermore, the track irregularity spectrum corresponds to the vertical irregularity of a single track or the vertical, horizontal, alignment, and rail gauge irregularities of double tracks, according to the selected plane or space vehicle model. In the above literature, accurate structural responses have been obtained using different vehicle load models. However, an overly refined vehicle and track model can result in low calculation efficiency. For comfort-based analysis, the selection of suitable vehicle load models to balance the calculation accuracy and efficiency remains to be investigated.

Table 1. Typical train load models and development objectives.

Development Objective	References
running safety	Ma et al., 2022 [27]; Zeng et al., 2022 [28]; Ju et al., 2023 [29]; Zhao et al., 2023 [30]; Tang et al., 2023 [31]; Li et al., 2024 [32]; Jiang et al., 2024 [33]
safety and durability of railways or bridges	Gou et al., 2023 [34]; Chen et al., 2024 [35]; Zhang et al., 2024 [36]
passenger comfort	Gou et al., 2023 [34]; Xin et al., 2023 [37]; Li et al., 2024 [32]
environmental vibration	Qu et al., 2022 [38]; Ren et al., 2023 [26]; Xu, 2023 [39]; Hu et al., 2024 [40]; Malmborg et al., 2024 [41]

2.1.2. Vibration Propagation in Soil and SSI

Buildings sensitive to vehicle-induced vibration can be classified as "vehicle-structure" and "vehicle-soil-structure" types based on the difference in the vibration propagation paths from the source to the structure. The difference between the two is whether the vibrations propagate primarily in the soil. The representative buildings of the first type include integrated station–bridge structures [42–45], buildings with carriageways inside [46,47], and railway overtrack buildings [48–50], among others. Their common characteristic in structural construction is that the track or carriageway is rigidly connected to the structure, and the vibration is primarily propagated within the structure. For instance, railway trains can cause comfort problems in waiting rooms and commercial areas within stations. Arriving and departing trains in stations have low speeds, and thus, integrated station–bridge structures will be more significantly impacted than the stations separated from rail bridges. The second type of building is characterized by vehicle-induced vibrations that must propagate in the soil and then into the structure. Buildings near railways

or roads mostly belong to this type [51,52]. This type of building is more common and numerous, and there are still frequent complaints and exceeded standards owing to current imperfections in environmental vibration assessment and structural design methods. For vehicle-induced vibrations in the second type of building, the vibration propagation behavior in the soil and SSI is critical.

The deformation of soil caused by vehicle-induced environmental vibrations is generally in the elastic phase. Waves in the soil are elastic waves that propagate as body and surface waves. This issue began with Lamb's work in 1904, that is, the wave solution for an elastic semi-infinite spatial body acting on its surface or interior using a point or line load [53]. Subsequent researchers considered more complex soil and vibration source properties to extend and deepen Lamb's problem and initially obtained a vehicle-induced vibration propagation attenuation law in soil layers [54–57]. However, the complex dynamic properties of soil, difficulty in detecting inhomogeneous soil layers, and effects of surrounding structures result in difficulties in calculations and predictions. Prediction methods for environmental vibration include empirical formulas [58,59], analytical or semi-analytical methods [60,61], and numerical simulations [62–65], among which the finite element model (FEM) is the more accurate and commonly used prediction method [63–65]. With further research, the modeling of the dynamic properties of natural soil has progressed from elastic bodies [53] to viscoelastic bodies [66], and then to saturated or unsaturated porous media [67]. Although these existing studies have effectively improved accuracy, soil models still have many assumptions compared to natural soils. At present, field measurements remain an effective approach for obtaining vibration attenuation laws for the geological conditions of a region. Therefore, the current environmental impact assessment (EIA) standard in China states that tests are preferentially used to obtain vibration attenuation laws over distance [68].

Vehicle-induced environmental vibrations were input from the structural foundation. Therefore, the SSI becomes a non-negligible issue in the calculations. The SSI issue initially received attention in seismic response analyses [69]. Compared to earthquakes, vehicle-induced environmental vibrations are mainly focused in the vertical direction and have smaller amplitudes and higher frequencies. Under these two excitations, the soil properties and contact relationships with the structural foundation are different. Currently, the impact of SSI in the context of vehicle-induced vibrations has not been adequately addressed. Most existing models assume that the SSI is negligible, with the soil and structure subsystems being uncoupled during calculations. This uncoupled approach is more suited to far-fault ground motions, where the receivers are distant from the source [70]. However, in the case of vehicle-induced vibration, shorter source–receiver distances and higher frequencies result in greater interaction [71,72]. The effects of SSI are mainly reflected in three aspects: changing the original vibration field, elastic boundaries on the structure, and coupled damping [63–75]. Yao et al. [76] calculated that the vibration of building floors could decrease by 10–12 dB when the nonlinear contact interaction between soil and building foundation is considered. The interaction is influenced by dynamic soil characteristics, structural foundation types, structural mass, source–receiver distances, among others [73,77,78]. Coulier et al. [77] investigated that the interaction can be significant when the source–receiver distance is smaller than the dilatational wavelength in the soil for underground railway tunnels, or smaller than six Rayleigh wavelength for railway track at grade, through a case study of a building on a shallow foundation. Numeric contact elements or simplified spring and damper components can be utilized to model the SSI. Aubry and Clouteau [79] proposed a sub-structuring approach to simulate the SSI, which has been applied to structural vibrations under traffic excitation. Pyl et al. [80] first studied the SSI using a 3D model under road traffic excitation. Colaço et al. [72] used the equivalent stiffness and damping method to consider SSI in calculating railway-induced vibrations.

Vibration propagation in soil and the SSI cause non-uniform excitation of vehicle vibration loads on the structure. Previously, uniform excitation methods have been used to

apply vibrations at the ground or structural bottom to a structure calculation model [81,82]. However, Hua et al. [83] indicated that the impact of non-uniform excitation should be considered when calculating the structural dynamic response induced by subways. The non-uniform excitation effect can result in differences in the distribution of structural responses, and its load model and calculation methods need to be studied further.

2.1.3. Simplified Calculation Approach

For comfort-based structural analyses, the primary shortcoming of current vehicle-induced vibration load models is the calculation efficiency rather than accuracy. The accuracy of the load models developed for vehicle comfort and track safety satisfied the requirements of structural comfort analyses. However, the large number of DOFs in soil FEM, the iterative method, and the short calculation time steps result in a large amount of computation and increase the difficulty of modeling, debugging, and calculation of the model, which makes it difficult to extend this calculation method to structural design.

To improve calculation efficiency, researchers have proposed solutions from several perspectives. Zeng et al. [84] proposed a time-integration analysis scheme for the vehicle–bridge-interaction problem to prove the computational efficiency of existing algorithms; Wang et al. [85] developed a multi-point synchronous algorithm to solute the large sparse linear equations of the train–track–soil coupled system, resulting in a five- to tenfold increase in computation efficiency; Touhei [86] proposed a 2.5-dimension (2.5D) FEM to use wave number transformations to track and soil along the line direction. However, this method is challenging to apply to building structures [87]. Currently, simplified load models and efficient calculation methods are pressing requirements.

2.2. Human-Induced Vibration

Human-induced vibrations are a dynamic response of structures to human activity. In this subsection, the human-induced load model, human–structure interaction (HSI), and crowd load model are presented.

2.2.1. Human-Induced Load Model and HSI

Several landmark events, such as the Millennium Bridge vibration event (London, UK, 2000) [8] and the Techno Mart building vibration event (Seoul, Republic of Korea, 2011) [88], have attracted extensive attention regarding the comfort problem induced by humans. Human-induced loads generally have a low intensity and thus cause significant dynamic responses by exciting structural resonance. Because the main frequency of human-induced loads is 1–3 Hz, light and flexible engineering structures, such as pedestrian bridges, connective corridors, large-span buildings, and cantilevered buildings, are the primary study subjects [89,90]. In the structural design of such buildings, it is recommended that the fundamental frequency of the structure should exceed 3 Hz, thus avoiding human-induced comfort problems [14,91]. Some studies have proposed that high-frequency floor slabs may also experience human-induced vibration comfort problems [92]; however, this phenomenon requires more engineering cases to be verified.

The human body is an adaptive system, and human behavior is intensely subjective and random, resulting in complex human-induced loads. The establishment of human-induced loads is based on experiments and statistics on human body dynamics parameter calibration and plantar force measurement with different body postures. Furthermore, HSI is a central issue in the study of human-induced vibrations [93]. In particular, when light and strong building materials are applied, the structural frequency decreases, and the ratio of human–structure mass increases, resulting in a more significant effect of HSI. The relevant tests indicate that humans can alter the mass distribution and damping of the structural dynamic system [94–97]. The coupling mechanism and applicable conditions remain to be addressed to develop simplified calculation methods for structural design.

By simplifying the dynamic characteristics of the human body and the HSI, researchers have developed human-induced load models that correspond to various human activities, including walking, running, jumping, and bouncing, among others [89,98,99]. Table 2 lists part of the typical human-induced load models. In particular, the vertical walking load is the most common type of human-induced load and has received the most attention from researchers [89]. The time history of walking force during single-foot landing is double-peaked "M" shapes, consistent with the physical process from heel landing to toe off the ground when walking. In the frequency domain, the walking force has main harmonic and multi-order subharmonic peaks. Types of load models include the Fourier series model, spring-mass-damping model, and bipedal walking model, among others, as listed in Table 2.

Table 2. Typical human-induced load models.

Human Activities	Model Type	Originator, Year
walking (vertical load)	Fourier series model	Zivanovic et al., 2007 [100]; Chen et al., 2014 [101]
	spring-mass-damping model	Silva et al., 2013 [102]; Shahabpoor et al., 2023 [103]
	bipedal walking model	Whittington et al., 2009 [104]; Kim et al., 2011 [105]; Qin et al. 2013 [106]
	multibody model	Máca et al., 2011 [107]
	power spectrum model	Brownjohn et al., 2004 [108]; Piccardo et al., 2012 [109]; Ferrarotti et al., 2016 [110]; Chen et al., 2019 [111]; Wang et al., 2020 [112]
walking (lateral load)	synchronization-based model	Fujino et al., 1993 [113]; Dallard et al., 2001 [114]; Nakamura et al., 2004 [115]; Strogatz et al., 2005 [116]; Blekherman, 2005 [9]; Piccardo et al., 2008 [117]
	self-excitation model	Pizzimenti et al., 2005 [118]; Ingólfsson et al., 2011 [119];
	inverted pendulum model	Macdonald, 2008 [120]; Bocian et al. [121]; Carroll et al., 2011 [122]
running	Fourier series model	Racic et al., 2014 [123]
jumping	Fourier series model	Ellis et al., 2004 [124]
	power spectrum model	Xiong et al., 2018 and 2021 [125,126];
bouncing	Fourier series model	Ji et al., 1994 [127]; Parkhouse et al. 2006 [128]; Duarte et al., 2009 [129]; Dougill et al., 2006 [130]; Wang et al., 2019 [131]
	SMD model	

The modeling of human-induced loads is generally based on tests performed on the rigid ground. However, when a human is in a vibrational environment or on a flexible structure, the plantar force can differ from the test results on rigid ground because of the HSI and the spontaneous regulation of the human body system [132]. This influencing factor should be studied to refine the existing human-induced load models.

Human-induced load models applied to residential buildings with common functions have been extensively studied. In recent years, people have expected buildings to have more functionality; therefore, the number of new-functional and comprehensive buildings has increased. A human-induced load model must correspond to a building function. For instance, some special-shaped landscape bridges require staircase walking loads [133]; comprehensive buildings with indoor gymnasiums require sports loads (e.g., basketball, badminton, and volleyball); and comprehensive buildings with performance halls inside require human wave and swing loads. With the promotion and construction of these new buildings, novel human-induced load models required for structural design have become a future research trend.

2.2.2. Crowd Load Model

Because of simplifications in modeling, existing single-human-induced load models cannot completely simulate the dynamic characteristics of the human body yet. However, the mass ratio of one single person to a structure is too small to induce comfort problems. In engineering, the comfort problems of buildings are generally caused by crowd load excitation. Therefore, to improve the accuracy of human-induced vibration calculations, the primary objective is to consider crowd behavior in load modeling instead of further refining the single-human model.

Human dynamic parameters are related to factors such as gender, age, height, and weight, and their distribution in a crowd is strongly random. Moreover, crowd behavior patterns are influenced by building functions, spatial arrangements, and unexpected events [134]. Researchers initially combined single-human models into a crowd model, considered the statistical laws of random factors, and used the Monte Carlo method for a time-domain analysis to calculate the structural response [135]. Methods in the traffic planning field, such as the discrete element theory (DET) [136] and the social force model [137,138], have been used to simulate pathways of crowd activity. However, time-domain load models exhibit natural disadvantages in stochastic analyses. The high computational cost of the Monte Carlo method makes it difficult to use. Presently, the development of time-domain crowd load models has stagnated.

Frequency-domain crowd load models represented by power spectrum models have become a trend because of their advantages in stochastic analyses [108–112,125,126,139,140]. Chen's team contributed outstanding research results using this method [111,112,125,126,140], and the proposed reaction spectrum method was adopted for China's building floor design standard [91]. However, for the current power spectrum model of crowd load, the influence of various random crowd behaviors and the effect of HSI need further consideration.

In addition, with emerging technologies, such as smartphones, big data, motion capture, and neural networks, human-induced load models based on big data have study and application prospects [15,139–142].

2.3. Wind-Induced Vibration

Wind-induced vibration is the dynamic response of a structure to fluctuating wind. Fluctuating wind loads are horizontal dynamic loads with random characteristics that act on building structures. Because of the fluid–structure interaction, the structural dynamic behavior caused by wind loads is complex and includes downwind and crosswind vibrations (e.g., vortex-induced vibration).

Researchers have conducted measurements and formulated different wind speed spectra, such as Karman, Davenport, Harris, Kaimal, and Simiu wind spectra, to analyze downwind vibrations. Among these, the Davenport wind spectrum is based on the measured data of multiple regions and, therefore, has wide applicability [143]. Equation (3) delineates the expression of the power spectrum $S_v(n)$. By using the wind speed spectrum, pulsating wind speeds can be simulated through methods like linear filtering, harmonic superposition, or other techniques. Subsequently, the pulsating wind pressure load is derived from the correlation between wind pressure and speed.

$$S_v(n) = 4K\bar{v}_{10}{}^2 \frac{x^2}{(1+x^2)^{4/3}} \quad (3)$$

where $x = 1200\,n/\bar{v}_{10}$; n is frequency; $\bar{v}_{10}$ is the mean hourly wind speed at the standard reference height of 10 m; K is the drag coefficient for the surface.

The complexity of crosswind vibrations and wind loads in tall buildings surpasses that of downwind vibrations, primarily due to factors like vortex-induced resonance. Developing a mathematical model that accurately describes vortex-induced forces is an effective approach to address this problem, albeit challenging. The complexity of vortex-induced vibrations stems from the shedding of wake vortices at different stages within

the lock-in range, and various structural boundary conditions lead to the emergence of different modes. Several simplified mathematical models for vortex-induced forces have been proposed. For instance, the Ruscheweyh model describes vortex-induced forces as harmonic forces [144] in Equation (4). However, the simple model lacks the representation of key properties of vortex-induced vibrations, such as the locking phenomenon and self-limiting amplitudes. Bishop [145], Tamura [146], Vickery [147], Ehsan [148], Larsen [149] et al. proposed more intricate and refined expressions to depict the relationship between frequency, amplitude, and phase of vortex-induced forces and structural parameters. The key fluid parameters in these models must be assumed in advance or identified from measured vortex-induced vibration responses of the structure. Currently, simulation based on computational fluid dynamics is the main technique to calculate vortex-induced forces [150,151].

$$F_v = \frac{1}{2}\rho V^2 D C_L \sin(\omega_s t + \varphi) \quad (4)$$

where F_v is the vortex-induced force; ρ is the density of air; V is the wind speed; D is the structural cross-section dimensions in crosswind direction; C_L is the root mean square of the lift coefficient; ω_s is the circular frequency; t is the time; φ is the phase difference between structural displacement response and vortex-induced force

Early research on the structural wind resistance design of high-rise buildings focused mainly on structural safety and less on comfort [152]. With the development of urban construction, the number of high-rise and super-high-rise structures is increasing, and wind-induced vibration comfort has often determined the structural design of these buildings. Studies of wind-induced vibration comfort have become increasingly critical.

Traditional methods for safety-based wind-resistant structural analysis are unsuitable for comfort-based analysis, and the understanding of wind-induced comfort calculation and evaluation methods has not been unified. The evaluation index in China uses the downwind and crosswind peak acceleration on top of structures [153,154], with the aim of controlling the vibration at the peak position of the structural first-order mode. However, the tops of high-rise or super-high-rise buildings are often unmanned activity rooftop platforms, masts for lightning protection, or antennae, where comfort problems do not occur. Moreover, wind loads can excite high-order modes of the structure under specific circumstances, which may result in maximum vibration occurring in the middle floors of the building. The ISO and some countries, such as Japan, stipulate that the maximum peak acceleration in the downwind and crosswind directions of all occupied floors must be evaluated [155,156]. In addition, the maximum direction of the wind-induced vibration requires further discussion. When the mass center of the structure does not coincide with the stiffness center, the structure has torsional vibration modes, and the maximum direction of the horizontal vibration can form an angle with the downwind and crosswind directions. Furthermore, under wind load excitation, vertical vibrations of the floor slabs occurred with horizontal vibrations because of the smaller out-of-plane stiffness of the slabs. Therefore, the vibration directions used for the evaluation, such as downwind, crosswind, maximum horizontal, vertical, or whole-body vibrations, require further determination.

The recent SEG Plaza building vibration event (Shenzhen, China, 2021) brought wind-induced comfort problems into public view and attracted the attention of researchers and engineers [157–160]. Experts investigated the event, and the cause was found to be the coupling of the vortex-induced resonance of the mast and the change in the dynamic characteristics of the building and the mast. This event may become a landmark in research on wind-induced vibration comfort. Discussing the vibration mechanism, structural analysis theory, evaluation methods, and other issues can significantly promote the study of wind-induced vibration comfort and update structural design and evaluation systems.

2.4. Machinery-Induced Vibration

Machinery-induced vibration is the dynamic response of structures to dynamic machinery. According to the function and use scenario, the possible machinery includes living equipment (elevators [161], water pumps, power transformers [162], and fans, among others), industrial production equipment (ball mills, bridge cranes [163], and punch machinery, among others), and engineering construction equipment (dynamic compaction machinery [164], rock excavation [165], and pile drivers, among others). Owing to the shortage of urban land and intensive building planning, the distance between this dynamic machinery and the living environment is gradually reduced, even inside buildings. In general, the load of dynamic machinery is not complex. However, different types of dynamic machinery have different characteristics in the time and frequency domains, and their corresponding load models and modeling techniques are also different. Based on the generation mechanism of machinery-induced vibrations and load characteristics, dynamic machinery loads can be divided into three types, and commonly used load modeling techniques are listed in Table 3.

Table 3. Dynamic machinery load types and modeling techniques.

Type No.	Machinery Examples	Generation Mechanism	Load Characteristic	Modeling Techniques
I	elevator traction machinery, power transformer, water pump, fan, ball mill	reciprocating or rotating mechanisms	smooth stochastic process; fixed frequency components; spectrum contains main and multi-order harmonic frequencies	simple harmonic forces; Fourier series model; power spectrum model
II	elevator car, bridge crane	machines move along fixed tracks or routes on the structure	moving load (related to mass, speed, track irregularities, and contact relationships)	moving force, multi-rigid body model
III	punch machinery, dynamic compaction machinery, pile driver	impact behavior during machinery operation	pulse load	impact force, impact process numerical simulation

There are fewer research cases involving dynamic machinery loads and induced structural dynamic response compared to the other categories of loads mentioned above, such as vehicle-induced and human-induced loads. Moreover, because of the large number of machinery categories, most machinery categories have not been developed into mature load models. In engineering, measured vibration data at the vibration source of machinery are used directly as the input. With people paying more attention to comfort problems, it is necessary to establish standardized load models for common dynamic machinery. In addition, structural calculation models, evaluation methods, and isolation measures for machinery-induced vibrations require further investigation.

3. Comfort-Based Structural Analysis Method

With the development of numerical simulation technology and the upgrading of computer performance, the FEM has become the mainstream method for dynamic analysis in structural design. Compared with safety-based structural simplification models for strong vibration analysis, comfort-based structural model simplification methods should be different.

Strong vibration analysis focuses on the bearing capacity or deformation properties of the main load-bearing skeleton of a structure under ultimate loads such as earthquakes. The purpose is to avoid the loss of the seismic or gravity-bearing capacity of the entire structure because of damage to parts of the structure or components. Instead, vibration comfort problems are within the scope of weak vibration analysis. This focuses on the serviceability of structures under micro-amplitude vibrations. Its purpose is to service the

people in the structure and consider the comfort of the people in the vibration environment as a criterion. Under micro-amplitude vibrations, the structure has small deformation and is in a state of linear elasticity. Therefore, the comfort-based model should reflect the dynamic characteristics of the objective structure under micro-amplitude vibrations and accurately calculate the acceleration of the floor where people are located. In addition, the median perception threshold of fit persons for the weighted acceleration peak magnitude is approximately 0.015 m/s^2 [166,167], indicating that the accuracy of comfort-based analysis should also achieve this magnitude.

Based on the above principles, He and Xie [168] proposed a sophisticated calculation model for large-span railway station structures based on the evaluation of vibration serviceability. Based on the strong vibration model of the structure, the method models the non-structural components, considers the local construction and boundary conditions, modifies the calculation parameters such as the live load coefficient and damping ratio, and finally obtains a refined elasticity FEM of the structure during the normal service state. Furthermore, by validating additional engineering structures, the modeling method can be suitable for more structural comfort problems [43,161,162]. The following subsection presents the critical differences between the comfort-based structural analysis model and the traditional strong vibration model.

3.1. Structural Floor Slab

The floor slab is the structural component where people are located and the source of the human body receiving vibrations, and therefore, is the location that standards specify for evaluation. The dynamic characteristic of structural floor slabs is an emphasis in modeling.

For a structural floor, a strong vibration model generally adopts the rigid floor assumption and ignores its out-of-plane stiffness. Instead, in comfort-based structural analysis, the main structure, including the structural floor slabs, must be simplified as elastic elements. Researchers have generally accepted this opinion and developed various elasticity calculation models [163,169]. Application of conventional modeling techniques has been shown to be adequate for typical floor slabs such as reinforced concrete slabs. However, novel slab materials or composite floor types have recently been developed with excellent performance and complex construction [170–172]. For each of these applications, it is necessary to study the dynamic behavior by developing suitable modeling techniques.

3.2. Non-Structural Components

Non-structural components are non-load-bearing components in the structural design, including flooring finishes, infill walls, and curtain walls, among others. Strong vibration models generally ignore the effects of non-structural components on the global stiffness and damping of the structure. The model simplified these components to additional mass or load composite values. Instead, when the structure is in a state of normal use, some non-structural components can change the structural mass, stiffness distribution, and damping properties, which can significantly affect the dynamic characteristics of the structure under micro-amplitude vibrations, thus affecting the dynamic response [173]. The influence of various non-structural components on the dynamic characteristics of structures has become a topic of interest [174]. Two types of non-structural components with significant impacts are the non-structural floor layer and wall, which are explained in the following.

- Non-structural layer of floors

The non-structural floor layer is the functional and decorative layer laid on the structural floor slab, such as a thermal insulation layer (foam board), levelling layer (cement mortar), and decorative surface layer (tiles, timber, marble, rubber, and elevated flooring). These non-structural layers may increase floor thickness by more than 50%. Research indicates that an insulation layer can significantly increase the damping ratio of floors [168].

Different materials and types of decorative surfaces have different effects on the dynamic characteristics of floor slabs [174–177]. These effects should be considered in the calculations to modify the dynamic characteristics of the floors.

- Non-structural wall

Non-structural walls, such as infill and curtain walls, have no load-bearing functions in their structural design. In comfort-based structural analysis, lightweight partition walls can be equivalently modeled in terms of mass and stiffness; infill walls can transmit interstory vibrations, increase the stiffness and damping of floors, alter the modal shapes [168,178], and increase the global lateral stiffness of the structure [179]; curtain walls have weak confinement effects between layers in addition to the effect of mass [180]. At present, the interaction mechanism between non-structural walls and the main structure remains to be investigated. Infill walls are constructed directly on the floor beams. Curtain walls are hung on the building facade using steel studs. The dynamic behavior of the connection between non-structural walls and the main structure is central to such studies. The connection stiffness and the vibration propagation law under weak vibration require further study.

In summary, the importance of non-structural components in comfort-based analyses has gradually been accepted and considered in modeling. However, the refined modeling for non-structural components increases the complexity of the numerical models and decreases the calculation efficiency. Non-structural components are varied and complex, and new component categories are constantly being developed and applied. Research on various non-structural components requires further discussion. Quantifying the effects of various non-structural components and developing simplified methods are practical approaches to consider non-structural components in structural design.

3.3. Local Construction and Boundary

Local constructions include window and door openings, structural joints, and bolted joints, among others. The vibration characteristics of these constructions under micro-amplitude vibrations differ from those under strong vibration conditions. For instance, window and door openings can decrease the mass and stiffness of the infill wall and alter its effect on the structural dynamic characteristics; structural joints under strong vibrations divide the structure completely, whereas those under micro-amplitude vibrations can transmit vibrations, and thus be simplified semi-rigid spring connections; trusses and bolted connections under strong vibration are considered to be axially loaded members and hinges, whereas the bolted nodes of trusses almost never rotate under micro-amplitude vibrations, thus be modeled as beam members and rigid or semi-rigid, respectively.

Modeling of the boundary depends on the selection of the calculation domain. Based on the vibration propagation features under different loads and structures, selecting the calculation domain and reasonably addressing the boundary can improve calculation efficiency while balancing accuracy requirements. For instance, the following can be performed: in vehicle-induced vibration, modeling the building structure and setting up equivalent stiffness and damping at the base of the structure to consider the SSI [78]; in human-induced vibration, modeling partial floors and constraining boundaries for calculations [169]; and in wind-induced vibration, modeling the superstructure, ignoring the foundations, and constraining the model bottom as the fixed end [157]. Current numerical models may have redundant parts that affect the calculation efficiency, and the vibration propagation mechanism requires further investigation.

3.4. Other Dynamic Parameters

This subsection adds other dynamic parameters that are not discussed above but should not be ignored in comfort-based structural analyses.

- Additional mass

Placing large-mass items on the floor, such as large decorations, fixed equipment, and furniture, can change the mass distribution and decrease the fundamental frequency of the floor [181].

- Dynamic elastic modulus

Elastic modulus can impact the natural frequency of structures, which is a key parameter in modeling [182,183]. In comfort-based structural analyses, the elastic modulus of the material at small deformations, that is, the dynamic elastic modulus, should be adopted. Compared to the static elastic modulus obtained by the axial compression experiment of prisms, the dynamic elastic modulus was obtained by the ultrasonic pulse method, representing the relationship between the stress and strain of the material under dynamic loading. For instance, the dynamic elastic modulus of concrete is greater than its static elastic modulus [184]. Bachmann et al. [12] proposed using the dynamic modulus of elasticity to predict the fundamental frequency of the floors in calculating human-induced vibration comfort. Therefore, the technical standard in China stipulates that for reinforced concrete floor or steel-concrete composite floor, the elastic modulus used in the calculation should be 1.2–1.35 times larger than the static elastic modulus to consider the dynamic elastic modulus [91].

- Damping ratio

Damping reduces the structural response. Structural damping mechanisms are complex, and the current theories are not fully comprehensive. In general structures, damping is mainly related to the material properties and other damper mechanisms used in the building. When a structure has great deformation transitioning from elasticity to plasticity, its damping can increase significantly. Consequently, the damping ratio in comfort-based structural analyses should be lower than in seismic analyses. Furthermore, even when structural deformation remains within the elastic range, the dissipation of damping energy during motion is influenced by the extent of deformation, thus exhibiting a relevance of the value of the damping ratio to the vibration amplitude [185,186]. Although a definitive relationship has yet to be established, it is generally observed that more minor excitation results in smaller vibration amplitudes, corresponding to a lower damping ratio. Therefore, in comfort-based structural analyses, the damping ratio under micro-amplitude vibration of the structure should be adopted, which is different from strong vibration analyses. Measured damping ratios of steel and concrete structures are generally about 0.01–0.02 during the normal service stage (micro-amplitude vibration) [168,182,187]. In addition, the wind-induced vibration of high-rise buildings is sensitive to the damping ratio. Hu et al. [157] measured a super-high-rise building and observed a sudden decrease in the damping ratio when wind-induced structural resonance occurred, which may be related to the aerodynamic damping effect [188].

- Construction and measurement error

Construction errors during the building process are common, such as those involving the properties of materials and the dimensions of beams, columns, and slabs. This results in the dynamic characteristic of a completed structure that differs from the design expectations. Construction errors are generally not considered in current structural modeling. In addition, ambient temperature changes can influence the dynamic characteristics of structures such as pedestrian bridges, resulting in fluctuations in the measured self-vibration frequency [189]. Wang et al. [190] monitored a reinforced concrete slab for over a year and observed that possible temperature changes of 0~50 °C can lead to an error of more than 15% in the self-vibration frequency of the tested slab. Errors in identifying structural dynamic characteristics and response measurements can impact the validation of structural models. Therefore, when the dynamic characteristics of the model are not consistent with the measurements, the effect of construction and measurement errors should be considered, in addition to the errors caused by modeling simplification and algorithms.

In summary, the comfort-based structural analysis aims to accurately calculate the vibration of the floors in the user activity area. Its principle is modeling the key members (component, connection, and boundary, among others) in detail and simplifying others based on the effect of each member under micro-amplitude vibration. However, this method has not yet covered all types of vibration sources, structures, or construction details, and a systematic method for structural design has not yet been developed.

4. Vibration Comfort Evaluation Method

Vibration comfort is based on human feelings, which are influenced by the following three categories of factors: (a) external vibration factors, including direction, frequency, amplitude, duration, and load return period; (b) external environmental factors, including structural-borne noise, airborne noise, rattling, movement of furniture, and visual effects (e.g., movement of hanging objects); and (c) receiver factors, including person type (gender, age, height, and health, among others), body posture, experience, expectation, activity motivation (e.g., ease or difficulty of the task performed), economic or living situation, and subjective ambiguity.

For these influencing factors, based on biodynamics, psychology, and fuzzy mathematics methods, researchers have statistically analyzed a large amount of test data, and their conclusions have been applied to comfort evaluations. The relationship between comfort and the amplitude and frequency of vibration acceleration has been studied in depth. The human body in buildings is sensitive to vibration in the 1–80 Hz range [191], and the ISO provides frequency weighting methods for vibrations in different directions and body postures [166,167]. Table 4 lists some of the comfort evaluation standards in various countries with their indexes and partial limits.

Table 4. Comfort evaluation standards in various countries.

Standard; Country, Region, or Organization	Vibration Source	Comfort Index	Evaluation Objects and Limits (Part)
ISO 2631-1: 1997; ISO [166,167]	-	RMS; VDV	uncomfortable: "RMS" 0.8 m/s^2 to 1.6 m/s^2
ISO 10137-2007; ISO [14]	vehicle; human; wind; machinery	RMS; VDV; PA	1. vibration induced by vehicles, humans, or machinery: "RMS, VDV" base curve × multiplying factor; 2. wind-induced vibration: "PA" frequency-dependent curve
ISO 6897-1984; ISO [156]	wind	RMS	frequency-dependent curve
GB 10070-88; China [192]	vehicle; machinery	VAL (VL_z)	residential, cultural and educational building (day): 70 dB
JGJ/T 441-2019; China [91]	human; machinery	PA	building floor with walking loads primarily (residential, hospital, office, etc.): 0.05 m/s^2
JGJ/T 170-2009; China [193]	vehicle	VAL (VL_{max})	residential, cultural and educational buildings (day): 65 dB
JGJ 3-2010; China [153]	wind	PA	concrete structure of tall buildings (residential, apartment): 0.15 m/s^2
JGJ 99-2015; China [154]	wind	PA	steel structure of tall buildings (apartment): 0.20 m/s^2
ATC Design Guide 1; USA [194]	human	RMS; PA	1. vertical vibration: "RMS" base curve × multiplying factor; 2. horizontal vibration (office, residential, etc.): "PA" 0.02 m/s^2
AISC Design Guide 11; USA [195]	human	PA	floor and pedestrian bridge: base curve × multiplying factor
EN 1990: 2002 [196]	human	PA	vertical vibration (pedestrian bridge): 0.7 m/s^2
BS 6472-1: 2008; UK [197]	-	VDV	residential building (16 h day): adverse comment possible 0.4 m/s$^{1.75}$ to 0.8 m/s$^{1.75}$

AIJ ES001-V001; Japan [198]	vehicle; human; wind; machinery	PA	building: frequency-dependent curve
AIJ-GEH-2004; Japan [155]	wind	PA	building: frequency-dependent curve

Note: RMS is weighted acceleration root mean square; VDV is vibration dose value; PA is peak acceleration; VAL is weighted vibration acceleration level, and Z-vibration level VL_z is weighted vertical VAL, frequency maximum magnitude of vibration VL_{max} is maximum weighted vertical VAL at the 1/3-octave center frequency.

From Table 4, the comfort indicators of the existing standards are not unified and use different limits, which lack the basis for conversion. Some indicators are tailored to specific application conditions, yet even for the same comfort issue, different indicators may exist. In engineering applications, using different standards can yield divergent assessment outcomes. These comfort evaluation indices can be classified into two categories. For vibrations with a single primary frequency, such as human-induced vibrations and wind-induced vibrations, peak acceleration is generally adopted [14,91,153–155,194–196,198], whereas broadband vibrations, such as vehicle-induced vibrations, are generally described as weighted acceleration root mean square $a_{\mathrm{w,RMS}}$, vibration dose value $a_{\mathrm{w,VDV}}$[14] or Z-vibration level VL_z [192], as expressed in Equations (5)–(7). Furthermore, when assessing the vibration comfort problems of floors and pedestrian bridges caused by humans, both natural frequency and peak acceleration are commonly employed [199]. For instance, the Chinese standard JGJ/T 441-2019 specifies that for the floor slabs in residential or office buildings primarily excited by walking loads, the first-order vertical self-vibration frequency should be over 3 Hz, and the limit of vertical peak acceleration is 0.05 m/s² [91].

$$a_{\mathrm{w,RMS}} = \left[\frac{1}{T}\int_0^T a_{\mathrm{w}}^2(t)\mathrm{d}t\right]^{1/2} \tag{5}$$

$$a_{\mathrm{w,VDV}} = \left[\frac{1}{T}\int_0^T a_{\mathrm{w}}^4(t)\mathrm{d}t\right]^{1/4} \tag{6}$$

where $a_{\mathrm{w}}(t)$ is the weighted acceleration as a function of time; T is the duration of the measurement.

$$VL_{\mathrm{z}} = 20\lg\frac{a_{\mathrm{w,RMS}}}{a_0} \tag{7}$$

where $a_0 = 10^{-6}\,\mathrm{m/s^2}$ is the reference acceleration.

Most existing evaluation standards do not consider or simplify the vibration duration and load return period of the influencing factors. In ISO 10137-2007, different multiplying factors are adopted for the "continuous vibration and intermittent vibration" and the "impulsive vibration excitation with several occurrences per day" [14], which demands more stringent limits for the first type of vibration source. The ISO standard published in 1985, ISO 2631-1:1985 Evaluation of human exposure to whole-body vibration-Part 1: General requirements (Withdrawn) [200], specified the evaluation limits for exposure times from 1 min to 24 h and an equation for the accumulation of exposure times for intermittent vibration. As the exposure time increases, a person's tolerance to vibration decreases, and the demand for limits becomes more stringent. However, this part was simplified in the revised version of ISO 2631-1:1997, and the definition of "fatigue-decreased proficiency" was removed [166,167]. Despite this, the influence of the vibration duration and load return period on comfort evaluation should not be ignored, and further refined evaluation methods are required.

In principle, the position of comfort evaluation should be located at the maximum vibration of floors in the user activity area, which is related to the load characteristics, load

locations, structure types, and building functions. However, the existing evaluation method requires further improvement because of insufficient conclusions regarding the location of the maximum vibration and the lag of the standards with respect to the latest research. The shortcomings include the following: (a) in vehicle-induced vibration, the spatial distribution of the response is uncertain, and the measured maximum locations can be observed on the lower [201,202], middle [203], or top floors [204–206]. Therefore, the influence of the structural global and floor local modes on the structural response requires discussion. (b) Comprehensive evaluation of multi-directional vibration requires consideration, such as the horizontal response induced by vehicles in high-rise buildings increases with height [207], and horizontal wind loads may cause vertical floor vibration. (c) The comfort evaluation limits for different types of structures should be unified. For example, China's wind vibration evaluation standards specify different peak acceleration limits for concrete and steel structures [153,154]. In addition, the vibration duration and load return period should be added to the comfort evaluation system.

Existing comfort tests have some shortcomings that require further refinements, such as insufficient sample capacity, the difficulty in artificially simulating vibration to accurately reflect the actual vibrations, consideration of the psychological state of the subject, the difficulty in quantifying the influence of external environmental factors, and the current lack of standardized test technology. With the widespread adoption of smartphones and the Internet, human body movements and comfort feelings can by conveniently recorded and then collected by uploading them to the cloud via the Internet. Deep learning and artificial intelligence provide efficient algorithms to train collected big data of the important factors under various influential factors [208–210]. Researchers have begun exploring of these emerging technologies in studying comfort indexes. For instance, Chen et al. [211] proposed a smartphone-based evaluation system for pedestrian-induced footbridge vibration comfort; Cao et al. [15,212] designed a smartphone-based application and an online big data approach to investigate vibration serviceability limits in real environments. In addition, the vibration acceleration of structures is an essential indicator for assessing vibration comfort and obtaining reliable acceleration signal data. Various test techniques developed for structural health monitoring could be used to enhance the comfort-based vibration testing approach [213,214].

5. Mitigation Measures for Vibration Comfort

When the structural response exceeds standard limits and can cause discomfort for building occupants, vibration mitigation measures must be implemented. Vibration control technology has mature theories and has evolved alongside the development of new materials and processes. The vibration sources that cause comfort problems lead to structural responses with small amplitudes and possibly high frequencies, making not all techniques or products for the earthquake-resistant design applicable. Depending on the presence or absence of external energy input, these measures can be categorized as active or passive control technologies. In micro-amplitude vibration control for comfort, passive control technology is primarily utilized. This section focuses on the commonly employed measures to address comfort issues, including vibration isolation in railway tracks, vibration isolation barriers in soil, vibration isolation bearings for building structures, and tuned mass dampers (TMD).

5.1. Vibration Isolation in Railway Tracks

Vibrations induced by vehicles and machinery are artificial vibration sources, making isolating these sources an effective control strategy. In railway tracks, many systematic vibration isolation applications have been implemented [215–217]. These isolators are typically installed at the rails, rail fastenings, rail slabs, or ballast beds to mitigate the propagation of vehicle-induced vibrations to the surrounding environment. In recent years, phononic crystal theory has been employed in the design of vibration control techniques.

For instance, Hu et al. [218] developed a periodic layered slab track structure. The currently applied vibration isolators are typically effective in attenuating high-frequency vibrations but exhibit limited efficacy in addressing low-frequency components, sometimes even amplifying such vibrations. Low-frequency vibrations demonstrate less attenuation through soil over distances compared to high-frequency vibrations additionally, increasing the risk of resonance with building structures possessing low-frequency natural frequencies. Consequently, enhancing the capacity of track vibration isolators to mitigate low-frequency vibrations has emerged as a primary imperative. Sung et al. [219] developed an additional anti-vibration sleeper track to reduce low-frequency vibrations. Qu et al. [220] introduced a railway track concept inspired by chiral phononic crystals, offering significantly improved low-frequency vibration isolation through an orthogonal polarization coupling mechanism within the chiral subunit cell. Although track vibration isolation measures have been commonly implemented in urban rail transit systems, their adoption in high-speed rail networks remains limited due to safety and durability concerns.

5.2. Vibration Isolation Barrier in Soil

Vibration isolation barriers are constructed within the soil to isolate propagation paths. This strategy is particularly relevant in scenarios involving vibrations generated by vehicles or machinery. Common types of vibration isolation barriers include in-filled trenches [221–223], arrays of piles [224], and wave-impeding blocks (WIB) [225–227], among others. Vibration waves exhibit phenomena such as reflection and diffraction upon encountering these barriers. Consequently, the dimensions of the barrier, including width, length, and depth, must be determined based on the wavelength and the dimensions of the vibration source and the sensitive structure. In recent years, the application of phononic crystal theory for analyzing wave behaviors in periodic structures has gained significant traction. For instance, Pu et al. [228] revisited the surface wave manipulation in periodic trench barriers from the perspective of complex band structures. A limitation of vibration isolation barriers is the large engineering quantity for construction, especially when targeting long wavelengths for isolation, which necessitates extensive lengths and depths. For example, fillers in in-filled trenches may encounter contamination or consolidation, diminishing the vibration mitigation effect.

5.3. Base Vibration Isolation Bearing

With the focus on comfort issues induced by railways and the construction of sensitive building structures like over-track buildings, there is a growing need for vibration isolation bearings to mitigate vehicle-induced vibrations. Traditional isolation bearings, such as laminated rubber bearings, lead rubber bearings, and friction pendulum bearings, have proven effective in mitigating horizontal ground motion caused by earthquakes. However, vehicle-induced vibrations primarily occur in the vertical direction. The mechanism of isolation bearings involves shifting the natural frequency of the superstructure to deviate from the primary frequency of ground motion [229]. Vehicle-induced excitation typically spans a broad frequency range, posing the challenge of frequency shifting. Initially, researchers investigated the impact of traditional seismic isolation bearings on vertical railway-induced vibration isolation [49,230,231]. Subsequently, the concept of integrated control of engineering and seismic vibrations in China has led to a surge in research interest in three-dimensional vibration isolation bearings (3D-VIB) that can effectively address both seismic and vehicle-induced vibrations [232]. Building upon traditional seismic bearings, researchers have proposed various innovative designs and configurations for these bearings. For instance, Cao and Pan et al. [233,234] developed a 3D-VIB using a combination of disc springs and single friction pendulum bearings and another design incorporating a thick laminated rubber bearing and a friction pendulum. Sheng et al. [235] developed a new 3D-VIB, which is a laminated rubber bearing with vertical through-holes filled by a mixture of sand and rubber particles. Liang et al. [236] proposed a 3D-VIB composed of rubber isolation bearings and disc springs. He et al. [237] proposed a hybrid

vibration bearing consisting of lead rubber bearing and thick rubber bearing with decoupled horizontal and vertical behaviors. While the aforementioned innovative vibration isolation bearings have demonstrated outstanding performance in both experimental and simulation settings, their practical application effects in engineering remain to be validated. In addition, isolation bearings intended for vehicle-induced vibrations must permit relative motion between the superstructure and substructure under daily micro-amplitude vibrations. It inevitably decreases horizontal stiffness and potentially raises risks of destabilization.

5.4. TMD in Building Structures

TMDs currently serve as a primary technology for mitigating wind-induced vibrations in super tall buildings, human-induced vibrations in large-span floors and pedestrian bridges [238,239], and occasionally, vibrations caused by machinery within structures [240]. The fundamental configuration of TMDs consists of a mass, springs, and dampers and is designed to absorb vibrations at specific frequencies. The target frequency is generally the horizontal first-order frequency for tall buildings or the vertical first-order frequency for floors and bridges. TMDs are installed at the location of the maximum amplitude of the mode shapes. The ratio between the TMD mass and the generalized mass of the to-be-controlled mode defines the maximum vibration reduction effect. Therefore, conventional TMDs often exhibit excessive mass, posing safety risks. Distributed tuned mass dampers (MTMD) have been proposed to address this issue, and additionally implemented for the control of multi-order structural modes [241]. With the development of new materials and processes, novel TMDs have been proposed, including: (a) TMDs with more complex DOFs, nonlinear stiffness components or novel dampers [242–245]; (b) semi-active tuned mass dampers (SATMDs) [246,247] and active rotary inertia driver (ARID) systems [248]; and (c) tuned mass damper inerters (TMDIs) [249]. Furthermore, the fixed-point law in classical Den Hartog theory has been widely adopted for engineering designs. Using the minimum acceleration of the original structure as the optimization criterion, Ikeda et al. [250] derived the optimal ratios of frequencies and damping ratios are

$$\gamma_{\text{opt}} = \frac{1}{1+\mu} + (0.096 + 0.88\mu - 1.8\mu^2)\xi + (1.34 - 2.9\mu + 3\mu^2)\xi^2 \quad (8)$$

$$\xi_{\text{opt}} = \sqrt{\frac{3\mu(1 + 0.49\mu + 3\mu^2)}{8(1+\mu)}} + (0.13 + 0.72\mu + 0.2\mu^2)\xi + (0.19 + 1.6\mu - 4\mu^2)\xi^2 \quad (9)$$

where γ_{opt} and ξ_{opt} are the optimal ratios of frequencies and damping ratios, respectively; μ is the mass ratio; ξ is the damping ratio of the structure.

Nevertheless, researchers have continued to investigate the location and parameters of the novel TMDs to optimize the adsorption effect and robustness, such as H_2 norm optimization [251]. In addition, despite the widespread adoption of TMD technology, its efficacy in vibration reduction occasionally falls short of engineering expectations due to various factors: low sensitivity of TMDs, which cannot be activated in case of micro-amplitude vibrations; malfunctions in critical components such as damper oil leaks; inaccurate prediction of structural frequency resulting in the deviation of the parameters of the pre-customized TMD from the optimal values.

6. Conclusions

Compared to traditional seismic and wind resistance analyses, vibration comfort remains a niche research direction. Nevertheless, it covers a broad scope and often involves collaboration across multiple disciplines and fields. In recent years, research on vibration comfort has progressed significantly, and calculation theories and evaluation methods have been established. However, there are still some issues to be addressed. This paper discusses recent developments in this field and presents the existing shortcomings in research

and applications. The following are suggested potential topics for future studies regarding the load, structural analysis, evaluation methods, and vibration mitigation measures.

1. Standardized stochastic load models

The main load categories that can cause vibration comfort problems are vehicle-induced, human-induced, fluctuating wind, and dynamic machinery loads. Current load models for structural design are not sufficiently developed for adoption. For fluctuating wind loads, mature power spectrum models have been established; for human-induced loads, relevant studies are ongoing; however, for the various types of dynamic machinery loads and the complex vibration source mechanism of vehicle-induced loads, widely accepted standardized stochastic load models are still lacking.

2. Simplified comfort-based modeling method for structural design

With increasing concern for vibration comfort problems, more building structures require specialised structural design and optimisation based on comfort. However, the current comfort-based modeling methods developed by researchers have not yet achieved the balance of convenience, accuracy, and efficiency required for structural design. Therefore, simplified comfort-based modeling methods for structural design have essential engineering applications.

3. Comfort evaluation method considering duration and load return period

Existing vibration comfort evaluations only consider the amplitude, frequency, and direction of vibration, and ignore other features, such as the vibration duration and load return period. As the types and forms of vibration sources increase, evaluation methodologies require further refinement.

4. Application of novel vibration mitigation measures

With the development of new materials (e.g., polymer materials, magnetorheological materials, and shape memory alloys), innovations in vibration isolator construction, and proposed corresponding vibration isolation design theories, vibration reduction and isolation measures have been upgraded and optimized. Researchers initially use theories, simulations, or experiments to innovate novel technologies and finally promote their application. However, many novel technologies have been devised without considering their implications on the safety and durability of the original structure, which should be emphasized.

Structural vibration comfort is a complex aspect of building design that requires careful consideration to ensure a comfortable environment for occupants. One possible approach is the installation of an alarm system that can monitor and notify managers and occupants of excessive structural vibrations. This system can help detect vibration sources within the building and effectively prevent secondary accidents, such as stampedes caused by excessive panic in crowds. The latest vibration-based structural health monitoring techniques could be feasibly utilized in the design of the system [252,253]. In addition, big data and machine-learning techniques also provide new ideas for research on structural vibration comfort and provide directions for future study. They can be useful in studying the stochastic behavior of loads and structures and the subjective ambiguity in comfort evaluation.

Author Contributions: Writing—original draft preparation, Y.H.; writing—review and editing, W.X. and Y.H.; supervision, W.X.; funding acquisition, W.X. All authors have read and agreed to the published version of the manuscript.

Funding: This research was funded by Natural Science Foundation of China, grant number 52278458.

Data Availability Statement: Data sharing is not applicable.

Conflicts of Interest: The authors declare no conflicts of interest.

References

1. Reiher, H.; Meister, F.J. Human sensitivity to vibrations. *Eng. Res.* **1931**, *2*, 381–386.
2. Miwa, T. Evaluation methods for vibration effect part 1: Measurements of threshold and equal sensation contours of whole body for vertical and horizontal vibrations. *Ind. Health* **1967**, *5*, 183–205.
3. Jones, A.J.; Saunders, D.J. Equal comfort contours for whole body vertical, pulsed sinusoidal vibration. *J. Sound Vib.* **1972**, *23*, 1–14. https://doi.org/10.1016/0022-460x(72)90785-7.
4. Irwin, A.W. Perception, comfort and performance criteria for human beings exposed to whole body pure yaw vibration and vibration containing yaw and translational. *J. Sound Vib.* **1981**, *76*, 481–497. https://doi.org/10.1016/0022-460X(81)90265-0.
5. Gierke, M.J. *Handbook of Human Vibration*; Academic Press: London, UK, 1990.
6. Kanda, J.; Tamura, Y.; Fujii, K.; Ohtsuki, T.; Shioya, K.; Nakata, S. Probabilistic evaluation of human perception threshold of horizontal vibration of buildings (0.125 Hz to 6.0 Hz). In Proceedings of the Structures Congress XII, Atlanta, GA, USA, 24–28 April 1994.
7. Shioya, K.; Fujii, K.; Tamura, Y.; Kanda, J. Human perception thresholds of two dimensional sinusoidal motion in horizontal plane. *J. Struct. Constr. Eng.* **1994**, *461*, 29–36. https://doi.org/10.3130/aijs.59.29_3.
8. Dallard, P.; Fitzpatrick, T.; Flint, A.; Low, A.; Roche, M. London Millennium bridge: Pedestrian-induced lateral vibration. *J. Bridge Eng.* **2001**, *6*, 412–417. https://doi.org/10.1061/(ASCE)1084-0702(2001)6:6(412).
9. Blekherman, A.N. Swaying of pedestrian bridges. *J. Bridge Eng.* **2005**, *10*, 142–150. https://doi.org/10.1061/ASCE1084-0702200510:2142.
10. Xia, H. *Traffic Induced Environment Vibrations and Controls*; Science Press: Beijing, China, 2010.
11. He, Y.; Zhang, Y.; Yao, Y.; He, Y.; Sheng, X. Review on the prediction and control of structural vibration and noise in buildings caused by rail transit. *Buildings* **2023**, *13*, 2310. https://doi.org/10.3390/buildings13092310.
12. Bachmann, H.; Ammann, W.J.; Deischl, F.; Eisenmann, J.; Floegl, I.; Hirsch, G.H.; Klein, G.K.; Lande, G.J.; Mahrenholtz, O.; Natke, H.G.; et al. *Vibration Problems in Structures: Practical Guidelines*; Birkhäuser: Basel, Switzerland, 1995. https://doi.org/10.1007/978-3-0348-9231-5.
13. *ISO 5805-1997*; Mechanical Vibration and Shock—Human Exposure—Vocabulary. International Organization for Standardization: Geneva, Switzerland, 1997.
14. *ISO 10137-2007*; Bases for Design of Structures—Serviceability of Buildings and Walkways against Vibrations. International Organization for Standardization: Geneva, Switzerland, 2007.
15. Cao, L.; Chen, J. Big data investigation for vibration serviceability using smart phones. *J. Vib. Eng.* **2020**, *33*, 961–970. https://doi.org/10.16385/j.cnki.issn.1004-4523.2020.05.011.
16. Willis, R. Preliminary essay to the appendix B: Experiments for determining the effects produced by causing weights to travel over bars with different velocities. In *Report of the Commissioners Appointed to Inquire into the Application of Iron to Railway Structures*; Grey, G., Ed.; W. Clowes and Sons: London, UK, 1849.
17. Stokes, G.G. Discussion of a differential equation relating to the breaking of railway bridges. *Trans. Camb. Philos. Soc.* **1849**, *8*, 707–735.
18. Yu, G.; Kiani, K.; Roshan, M. Dynamic analysis of multiple-nanobeam-systems acted upon by multiple moving nanoparticles accounting for nonlocality, lag, and lateral inertia. *Appl. Math. Model.* **2022**, *108*, 326–354. https://doi.org/10.1016/j.apm.2022.03.027.
19. Ma, X.; Roshan, M.; Kiani, K.; Nikkhoo, A. Dynamic response of an elastic tube-like nanostructure embedded in a vibrating medium and under the action of moving nano-objects. *Symmetry* **2023**, *15*, 1827. https://doi.org/10.3390/sym15101827.
20. Chu, K.H.; Garg, V.K.; Dhar, C.L. Railway-bridge impact: Simplified train and bridge model. *J. Struct. Div.* **1979**, *105*, 1823–1844. https://doi.org/10.1088/0031-9155/25/5/015.
21. Zhai, W.M. *Vehicle-Track Coupled Dynamics*; Science Press: Beijing, China, 2015; Volume 1.
22. Lei, X.Y. *High Speed Railway Track Dynamics: Models, Algorithms and Application*; Science Press: Beijing, China, 2022.
23. Luo, J.; Zhu, S.; Zhai, W.; An advanced train-slab track spatially coupled dynamics model: Theoretical methodologies and numerical applications. *J. Sound Vib.* **2021**, *501*, 116059. https://doi.org/10.1016/j.jsv.2021.116059.
24. Ma, M.; Liu, W.; Qian, C.; Deng, G.; Li, Y. Study of the train-induced vibration impact on a historic bell tower above two spatially overlapping metro lines. *Soil Dyn. Earthq. Eng.* **2016**, *81*, 58–74. https://doi.org/10.1016/j.soildyn.2015.11.007.
25. Qu, S.; Yang, J.; Zhu, S.; Zhai, W.; Kouroussis, G. A hybrid methodology for predicting train-induced vibration on sensitive equipment in far-field buildings. *Transp. Geotech.* **2021**, *31*, 100682. https://doi.org/10.1016/j.trgeo.2021.100682.
26. Ren, Y.; Qu, S.; Yang, J.; Li, Q.; Zhu, B.; Zhai, W.; Zhu, S. An efficient three-dimensional dynamic stiffness-based model for predicting subway train-induced building vibrations. *J. Build. Eng.* **2023**, *76*, 107239. https://doi.org/10.1016/j.jobe.2023.107239.
27. Ma, C.; Choi, D.H. Stochastic dynamic analysis of the train-track-bridge system under tridirectional spatially correlated ground motions. *Soil Dyn. Earthq. Eng.* **2022**, *160*, 107324. https://doi.org/10.1016/j.soildyn.2022.107324.
28. Zeng, Z.P.; Liu, F.S.; Wang, W.D. Three-dimensional train-track-bridge coupled dynamics model based on the explicit finite element method. *Soil Dyn. Earthq. Eng.* **2022**, *153*, 0267–7261. https://doi.org/10.1016/j.soildyn.2021.107066.
29. Ju, S.H. Derailment of high-speed trains moving on curved and cant rails under seismic loads. *Soil Dyn. Earthq. Eng.* **2023**, *166*, 107757. https://doi.org/10.1016/j.soildyn.2023.107757.
30. Zhao, H.; Wei, B.; Shao, Z.; Xie, X.; Jiang, L.; Xiang, P. Assessment of train running safety on railway bridges based on velocity-related indices under random near-fault ground motions. *Structures* **2023**, *57*, 105244. https://doi.org/10.1016/j.istruc.2023.105244.

31. Tang, Y.; Zhu, Z.; Ba, Z.; Lee, V.W.; Gong, W. Running safety assessment of trains considering post-earthquake damage state of bridge-track system. *Eng. Struct.* **2023**, *287*, 116187. https://doi.org/10.1016/j.engstruct.2023.116187.
32. Li, Z.; Xu, L.; Wang, W.; Zhang, J.; Wang, J.; Peng, B.; Zeng, Z. On use of train-track-subgrade dynamic model for investigating the train-induced cumulative deformation of subgrade and its dynamic effects. *Appl. Math. Model.* **2024**, *127*, 71–95. https://doi.org/10.1016/j.apm.2023.11.026.
33. Jiang, Y.; Chi, M.; Yang, J.; Dai, L.; Xie, Y.; Guo, Z. Investigation on the mechanism and measures of derailment of empty freight train passing a turnout in the diverging route. *Eng. Fail. Anal.* **2024**, *156*, 107822. https://doi.org/10.1016/j.engfailanal.2023.107822.
34. Gou, H.; Gao, H.; Ban, X.; Meng, X.; Bao, Y. Vibration energy transmission in high-speed train-track-bridge coupled systems. *Eng. Struct.* **2023**, *297*, 117019. https://doi.org/10.1016/j.engstruct.2023.117019.
35. Chen, L.; Wang, Y.; He, Z.; Zhai, Z.; Bai, Y. Research on dynamic characteristics of railway side-cracked slab for train-track coupled system. *Eng. Fail. Anal.* **2024**, *160*, 108241. https://doi.org/10.1016/j.engfailanal.2024.108241.
36. Zhang, Q.; Dong, J.; Leng, W.; Zhang, C.; Wen, C.; Zhou, Z. Dynamic stress response in a novel prestressed subgrade under heavy-haul train loading: A numerical analysis. *Constr. Build. Mater.* **2024**, *412*, 134749. https://doi.org/10.1016/j.conbuildmat.2023.134749.
37. Xin, T.; Wang, J.; Fang, Q.; Mai, H.; Guo, P.; Wang, G. Passenger ride comfort in subway due to new subway excavation below. *Tunn. Undergr. Space Technol.* **2023**, *132*, 104904. https://doi.org/10.1016/j.tust.2022.104904.
38. Qu, S.; Yang, J.; Feng, Y.; Peng, Y.; Zhao, C.; Zhu, S.; Zhai, W. Ground vibration induced by maglev trains running inside tunnel: Numerical modelling and experimental validation. *Soil Dyn. Earthq. Eng.* **2022**, *157*, 107278. https://doi.org/10.1016/j.soildyn.2022.107278.
39. Xu, L. An isoparametric element permutation method for railway tunnel-soil interaction modeling in train-track-tunnel-soil dynamic analysis. *Tunn. Undergr. Space Technol.* **2023**, *140*, 105320. https://doi.org/10.1016/j.tust.2023.105320.
40. Hu, J.; Zou, C.; Liu, Q.; Li, X.; Tao, Z. Floor vibration predictions based on train-track-building coupling model. *J. Build. Eng.* **2024**, *89*, 109340. https://doi.org/10.1016/j.jobe.2024.109340.
41. Malmborg, J.; Flodén, O.; Persson, P.; Persson, K. Numerical study on train-induced vibrations: A comparison of timber and concrete buildings. *Structures* **2024**, *62*, 106215. https://doi.org/10.1016/j.istruc.2024.106215.
42. Zhang, X.; Ruan, L.; Zhao, Y.; Zhou, X.; Li, X. A frequency domain model for analysing vibrations in large-scale integrated building-bridge structures induced by running trains. *Proc. ImechE Part F J. Rail and Rapid Transit* **2019**, *234*, 226–241. https://doi.org/10.1177/0954409719841793.
43. Xie, W.; Fang, S.; He, W.; Chen, B. Vibration serviceability evaluation of large-span station structures. In Proceedings of the 5th International Symposium on Environmental Vibration (ISEV2011), Chengdu, China, 20–22 October 2011.
44. Guo, X.; Wang, S. Research on the dynamic response of the multi-line elevated station with "integral station-bridge system". *Buildings* **2024**, *14*, 758. https://doi.org/10.3390/buildings14030758.
45. Wang, T.; Jiang, B.; Sun, X. Train-induced vibration prediction and control of a metro depot and over-track buildings. *Buildings* **2023**, *13*, 1995. https://doi.org/10.3390/buildings13081995.
46. Pridham, B.; Walters, N.; Nelson, L.; Roeder, B. Addressing Parking Garage Vibrations for the Design of Research and Healthcare Facilities. In *Dynamics of Civil Structures*; Caicedo, J., Pakzad, S., Eds.; The Society for Experimental Mechanics, Inc.: Danbury, CT, USA, 2017; pp. 147–157.
47. Pan, T.C.; Mita, A.; Li, J. Vehicle-induced floor vibrations in a multistory factory building. *J. Perform. Constr. Fac.* **2001**, *15*, 54–61. https://doi.org/10.1061/(asce)0887-3828(2001)15:2(54).
48. Tao, Z.; Moore, J.A.; Sanayei, M.; Wang, Y.; Zou, C. Train-induced floor vibration and structure-borne noise predictions in a low-rise over-track building. *Eng. Struct.* **2022**, *255*, 113914. https://doi.org/10.1016/j.engstruct.2022.113914.
49. Zhou, Y.; Ma, K.; Chen, P.; Lu, D.; Wu, H. Investigations on train-induced vibration and vibration control of an over-track building using thick-layer rubber bearings. *Struct. Des. Tall Spec. Build.* **2022**, *31*, e1898. https://doi.org/10.1002/tal.1898.
50. Zou, C.; Wang, Y.; Moore, J.A.; Sanayei, M. Train-induced field vibration measurements of ground and over-track buildings. *Sci. Total Environ.* **2016**, *575*, 1339–1351. https://doi.org/10.1016/j.scitotenv.2016.09.216.
51. He, L.; Tao, Z. Building vibration measurement and prediction during train operations. *Buildings* **2024**, *14*, 142. https://doi.org/10.3390/buildings14010142.
52. Haladin, I.; Bogut, M.; Lakušić, S. Analysis of tram traffic-induced vibration influence on earthquake damaged buildings. *Buildings* **2021**, *11*, 590. https://doi.org/10.3390/buildings11120590.
53. Lamb, H. On the propagation of tremors over the surface of an elastic solid. *Philo. Trans. R. Soc. Lond. Ser. A—Math. Phys. Eng. Sci.* **1903**, *72*, 128–130. https://doi.org/10.1098/rsta.1904.0013.
54. Gao, G.Y.; Song, J.; Yang, J. Identifying the boundary between near field and far field in ground vibration caused by surface loading. *J. Cent. South Univ.* **2014**, *21*, 3284–3294. https://doi.org/10.1007/s11771-014-2301-0.
55. Kim, D.S.; Lee, J.S. Propagation and attenuation characteristics of various ground vibrations. *Soil Dyn. Earthq. Eng.* **2000**, *19*, 115–126. https://doi.org/10.1016/S0267-7261(00)00002-6.
56. Niu, D.; Deng, Y.; Mu, H.; Chang, J.; Xuan, Y.; Cao, G. Attenuation and propagation characteristics of railway load-induced vibration in a loess area. *Transp. Geotech.* **2022**, *37*, 100858. https://doi.org/10.1016/j.trgeo.2022.100858.
57. Yang, Y.B.; Hung, H.H. Soil vibrations caused by underground moving trains. *J. Geotech. Geoenviron. Eng.* **2008**, *134*, 1633–1644. https://doi.org/10.1061/(ASCE)1090-0241(2008)134:11(1633).

58. Sadeghi, J.; Esmaeili, M.H.; Akbari, M. Reliability of FTA general vibration assessment model in prediction of subway induced ground borne vibrations. *Soil Dyn. Earthq. Eng.* **2019**, *117*, 300–311. https://doi.org/10.1016/j.soildyn.2018.11.002.
59. With, C.; Bahrekazemi, M.; Bodare, A.; Validation of an empirical model for prediction of train-induced ground vibrations. *Soil Dyn. Earthq. Eng.* **2006**, *26*, 983–990. https://doi.org/10.1016/j.soildyn.2006.03.005.
60. Cao, Z.G.; Cai, Y.Q.; Sun, H.L.; Xu, C.J. Dynamic responses of a poroelastic half-space from moving trains caused by vertical track irregularities. *Int. J. Numer. Anal. Meth. Geomech.* **2011**, *35*, 761–786. https://doi.org/10.1002/nag.919.
61. Sheng, X.; Jones, C.J.C.; Thompson, D.J. A theoretical model for ground vibration from trains generated by vertical track irregularities. *J. Sound Vib.* **2004**, *272*, 937–965. https://doi.org/10.1016/S0022-460X(03)00782-X.
62. Hussein, M.F.M.; Hunt, H.E.M. A numerical model for calculating vibration from a railway tunnel embedded in a full-space. *J. Sound Vib.* **2007**, *305*, 401–431. https://doi.org/10.1016/j.jsv.2007.03.068.
63. Degrande, G.; Clouteau, D.; Othman, R.; Arnst, M.; Chebli, H.; Klein, R.; Chatterjee, P.; Janssens, B. A numerical model for ground-borne vibrations from underground railway traffic based on a periodic finite element-boundary element formulation. *J. Sound Vib.* **2006**, *293*, 645–666. https://doi.org/10.1016/j.jsv.2005.12.023.
64. Xu, L.; Zhai, W. Vehicle-track-tunnel dynamic interaction: A finite/infinite element modelling method. *Railw. Eng. Sci.* **2021**, *29*, 109–126. https://doi.org/10.1007/s40534-021-00238-x.
65. Ma, M.; Xu, L.; Du, L.; Wu, Z.; Tan, X. Prediction of building vibration induced by metro trains running in a curved tunnel. *J. Vib. Control* **2020**, *27*, 515–528. https://doi.org/10.1177/1077546320930910.
66. Yang, Y.B.; Hung, H.H. A 2.5D finite/infinite element approach for modelling visco-elastic bodies subjected to moving loads. *Int. J. Numer. Methods Eng.* **2001**, *51*, 1317–1336. https://doi.org/10.1002/nme.208.
67. Biot, M.A. Generalized theory of acoustic propagation in porous dissipative media. *J. Acoust. Soc. Am.* **1962**, *34*, 1254–1264. https://doi.org/10.1121/1.1918315.
68. *HJ 453-2018*; Technical Guidelines for Environmental Impact Assessment—Urban Rail Transit. Ministry of Ecological Environment: Beijing, China, 2019.
69. Anand, V.; Kumar, S.R.S. Seismic soil-structure interaction: A state-of-the-art review. *Structures* **2018**, *16*, 317–326. https://doi.org/10.1016/j.istruc.2018.10.009.
70. Bielak, J.; Loukakis, K.; Hisada, Y.; Yoshimura, C. Domain reduction method for three-dimensional earthquake modeling in localized regions, part I: Theory. *Bull. Seism. Soc. Am.* **2003**, *93*, 817–824. https://doi.org/10.1785/0120010251.
71. Lopes, P.; Costa, P.A.; Ferraz, M.; Calçada, R.; Cardoso, A.S. Numerical modeling of vibrations induced by railway traffic in tunnels: From the source to the nearby buildings. *Soil Dyn. Earthq. Eng.* **2014**, *61*, 269–285. https://doi.org/10.1016/j.soildyn.2014.02.013.
72. Colaço, A.; Barbosa, D.; Costa, P.A. Hybrid soil-structure interaction approach for the assessment of vibrations in buildings due to railway traffic. *Transp. Geotech.* **2022**, *32*, 100691. https://doi.org/10.1016/j.trgeo.2021.100691.
73. Kuo, K.A.; Papadopoulos, M.; Lombaert, G.; Degrande, G. The coupling loss of a building subject to railway induced vibrations: Numerical modelling and experimental measurements. *J. Sound Vib.* **2019**, *442*, 459–481. https://doi.org/10.1016/j.jsv.2018.10.048.
74. Li, X.; Chen, Y.; Zou, C.; Wu, J.; Shen, Z.; Chen, Y. Building coupling loss measurement and prediction due to train-induced vertical vibrations. *Soil Dyn. Earthq. Eng.* **2023**, *164*, 107644. https://doi.org/10.1016/j.soildyn.2022.107644.
75. Edirisinghe, T.L.; Talbot, J.P. The significance of source-receiver interaction in the response of piled foundations to ground-borne vibration from underground railways. *J. Sound Vib.* **2021**, *506*, 116178. https://doi.org/10.1016/j.jsv.2021.116178.
76. Yao, J.B.; Xia, H.; Zhan, N. Study on the train-induced environmental vibrations considering soil-structure interaction. *Procedia Eng.* **2017**, *199*, 2747–2752. https://doi.org/10.1016/j.proeng.2017.09.303.
77. Coulier, P.; Lombaert, G.; Degrande, G. The influence of source-receiver interaction on the numerical prediction of railway induced vibrations. *J. Sound Vib.* **2014**, *333*, 2520–2538. https://doi.org/10.1016/j.jsv.2014.01.017.
78. Colaço, A.; Costa, P.A.; Castanheira-Pinto, A.; Amado-Mendes, P.; Calçada, R. Experimental validation of a simplified soil-structure interaction approach for the prediction of vibrations in buildings due to railway traffic. *Soil Dyn. Earthq. Eng.* **2020**, *141*, 106499. https://doi.org/10.1016/j.soildyn.2020.106499.
79. Aubry, D.; Clouteau, D. A Subdomain Approach to Dynamic Soil-structure Interaction. In *Recent Advances in Earthquake Engineering and Structural Dynamics*; Davidovici, D., Clough, R.W., Eds.; Ouest Editions/AFPS: Nantes, France, 1992; pp. 251–272.
80. Pyl, L.; Degrande, G.; Clouteau, D. Validation of a source-receiver model for road traffic induced vibrations in buildings. II: Receiver model. *J. Eng. Mech.* **2004**,*130*, 1394–1406. https://doi.org/10.1061/(ASCE)0733-9399(2004)130:12(1394).
81. Ling, Y.; Zhang, Y.; Luo, Q.; He, A. Field measurement and simplified numerical model for vibration response of subway superstructure. *Structures* **2023**, *47*, 313–323. https://doi.org/10.1016/j.istruc.2022.11.048.
82. Erkal, A.; Kocagöz, M.S. Interaction of vibrations of road and rail traffic with buildings and surrounding environment. *J. Perform. Constr. Facil.* **2020**, *34*, 04020038. https://doi.org/10.1061/(ASCE)CF.1943-5509.0001442.
83. Hua, Y.; Xie, W.; Xie, J.; Non-uniform excitation method for predicting railway-induced vibrations of buildings near operational subways. *J. Build. Eng.* **2024**, *84*, 108669. https://doi.org/10.1016/j.jobe.2024.108669.
84. Zeng, Q.; Stoura, C.D.; Dimitrakopoulos, E.G. A localised lagrange multipliers approach for the problem of vehicle-bridge-interaction. *Eng. Struct.* **2018**, *168*, 82–92. https://doi.org/10.1016/j.engstruct.2018.04.040.
85. Wang, L.; Zhu, Z.; Bai, Y.; Li, Q.; Costa, P.A.; Yu, Z. A fast random method for three-dimensional analysis of train-track-soil dynamic interaction. *Soil Dyn. Earthq. Eng.* **2018**, *115*, 252–262. https://doi.org/10.1016/j.soildyn.2018.08.021.

86. Touhei, T. Impulsive response of an elastic layered medium in the anti-plane wave field based on a thin-layered element and discrete wave number method. *Doboku Gakkai Ronbunshu* **1993**, *465*, 137–144. https://doi.org/10.2208/jscej.1993.465_137.
87. Yang, Y.B.; Ge, P.; Li, Q.; Liang, X.; Wu, Y. 2.5D vibration of railway-side buildings mitigated by open or infilled trenches considering rail irregularity. *Soil Dyn. Earthq. Eng.* **2018**, *106*, 204–214. https://doi.org/10.1016/j.soildyn.2017.12.027.
88. Lee, S.H.; Lee, K.K.; Woo, S.S.; Cho, S.H. Global vertical mode vibrations due to human group rhythmic movement in a 39 story building structure. *Eng. Struct.* **2013**, *57*, 296–305. https://doi.org/10.1016/j.engstruct.2013.09.035.
89. Chen, J. *Human-induced Load and Structural Vibration*; Science Press: Beijing, China, 2016.
90. Wang, H.; Ge, Q.; Zeng, D.; Zhang, Z.; Chen, J. Human-induced vibration serviceability: From dynamic load measurement towards the performance-based structural design. *Buildings* **2023**, *13*, 2075–5309. https://doi.org/10.3390/buildings13081977.
91. *JGJ/T 441-2019*; Technical Standard for Human Comfort of the Floor Vibration. Ministry of Housing and Urban-Rural Development: Beijing, China, 2019.
92. Mohammed, A.S.; Pavic, A.; Racic, V. Improved model for human induced vibrations of high-frequency floors. *Eng. Struct.* **2018**, *168*, 950–966. https://doi.org/10.1016/j.engstruct.2018.04.093.
93. Shahabpoor, E.; Pavic, A.; Racic, V. Interaction between walking humans and structures in vertical direction: A literature review. *Shock Vib.* **2016**, *2016*, 3430285. https://doi.org/10.1155/2016/3430285.
94. Salyards, K.A.; Noss, N.C. Experimental evaluation of the influence of human-structure interaction for vibration serviceability. *J. Perform. Constr. Facil.* **2014**, *28*, 458–465. https://doi.org/10.1061/(ASCE)CF.1943-5509.0000436.
95. Shahabpoor, E.; Pavic, A.; Racic, V.; Zivanovic, S. Effect of group walking traffic on dynamic properties of pedestrian structures. *J. Sound Vib.* **2017**, *387*, 207–225. https://doi.org/10.1016/j.jsv.2016.10.017.
96. Zhang, S.; Xu, L.; Qin, J. Vibration of lightweight steel floor systems with occupants: Modelling, formulation and dynamic properties. *Eng. Struct.* **2017**, *147*, 652–665. https://doi.org/10.1016/j.engstruct.2017.06.008.
97. Zhou, D.; Ji, T. Free vibration of rectangular plates with continuously distributed spring-mass. *Int. J. Solids Struct.* **2006**, *43*, 6502–6520. https://doi.org/10.1016/j.ijsolstr.2005.12.005.
98. Racic, V.; Pavic, A.; Brownjohn, J.M.W. Experimental identification and analytical modelling of human walking forces: Literature review. *J. Sound Vib.* **2009**, *326*, 1–49. https://doi.org/10.1016/j.jsv.2009.04.020.
99. Nikooyan, A.A.; Zadpoor, A.A. Mass-spring-damper modelling of the human body to study running and hopping—An overview. *Proc. IMechE Part H J. Eng. Med.* **2011**, *225*, 1121–1135. https://doi.org/10.1177/0954411911424210.
100. Živanović, S.; Pavić, A. Probability-based prediction of multi-mode vibration response to walking excitation. *Eng. Struct.* **2007**, *29*, 942–954. https://doi.org/10.1016/j.engstruct.2006.07.004.
101. Chen, J.; Wang, H.Q.; Peng, Y.X. Experimental investigation on fourier-series model walking load and its coefficients. *J. Vib. Shock.* **2014**, *33*, 11–15. https://doi.org/10.13465/j.cnki.jvs.2014.08.003.
102. Silva, F.T.D.; Brito, H.M.B.F.; Pimentel, R.L. Modeling of crowd load in vertical directiong using biodynamic model for pedestrians crossing footbridges. *Can. J. Civ. Eng.* **2013**, *40*, 1196–1204. https://doi.org/10.1139/cjce-2011-0587.
103. Shahabpoor, E.; Pavic, A. Human-structure dynamic interactions: Identification of two-degrees-of-freedom walking human model. *J. Sound Vib.* **2023**, *569*, 117974. https://doi.org/10.1016/j.jsv.2023.117974.
104. Whittington, B.R.; Thelen, D.G. A simple mass-spring model with roller feet can induce the ground reactions observed in human walking. *J. Biomech. Eng.* **2009**, *131*, 011013. https://doi.org/10.1115/1.3005147.
105. Kim, S.; Park, S. Leg stiffness increases with speed to modulate gait frequency and propulsion energy. *J. Biomech.* **2011**, *44*, 1253–1258. https://doi.org/10.1016/j.jbiomech.2011.02.072.
106. Qin, J.W.; Law, S.S.; Yang, Q.S.; Yang, N. Pedestrian-bridge dynamic interaction, including human participation. *J. Sound Vib.* **2013**, *332*, 1107–1124. https://doi.org/10.1016/j.jsv.2012.09.021.
107. Máca, J.; Valášek, M. Interaction of human gait and footbridges. In Proceedings of the 8th International Conference on Structural Dynamics (EURODYN 2011), Leuven, Belgium, 4–6 July 2011.
108. Brownjohn, J.M.W.; Pavic, A.; Omenzetter, P. A spectral density approach for modelling continuous vertical forces on pedestrian structures due to walking. *Can. J. Civ. Eng.* **2004**, *31*, 65–77. https://doi.org/10.1139/L03-072.
109. Piccardo, G.; Tubino, F. Equivalent spectral model and maximum dynamic response for the serviceability analysis of footbridges. *Eng. Struct.* **2012**, *40*, 445–456. https://doi.org/10.1016/j.engstruct.2012.03.005.
110. Ferrarotti, A.; Tubino, F. Generalized equivalent spectral model for serviceability analysis of footbridges. *J. Bridge Eng.* **2016**, *21*, 04016091. https://doi.org/10.1061/(ASCE)BE.1943-5592.0000963.
111. Chen, J.; Wang, J.; James, M.W.B. Power spectral-density model for pedestrian walking load. *J. Struct. Eng.* **2019**, *145*, 04018239. https://doi.org/10.1061/(ASCE)ST.1943-541X.0002248.
112. Wang, J.; Chen, J.; Yokoyama, Y.; Xiong, J. Spectral model for crowd walking load. *J. Struct. Eng.* **2020**, *146*, 04019220. https://doi.org/10.1061/(ASCE)ST.1943-541X.0002514.
113. Fujino, Y.; Pacheco, B.M.; Nakamura, S.; Warnitchai, P. Synchronization of human walking observed during lateral vibration of a congested pedestrian bridge. *Earthq. Eng. Struct. Dyn.* **1993**, *22*, 741–758. https://doi.org/10.1002/eqe.4290220902.
114. Dallard, P.; Fitzpatrick, A.J.; Flint, A.; Bourva, S.L.; Low, A.; Smith, R.M.R.; Willford, M. The London Millennium footbridge. *Struct. Eng.* **2001**, *79*, 17–33.
115. Nakamura, S. Model for lateral excitation of footbridges by synchronous walking. *J. Struct. Eng.* **2004**, *130*, 32–37. https://doi.org/10.1061/(ASCE)0733-9445(2004)130:1(32).

116. Strogatz, S.H.; Abrams, D.M.; McRobie, A.; Eckhardt, B.; Ott, E. Crowd synchrony on the Millennium bridge. *Nature* **2005**, *438*, 43–44. https://doi.org/10.1038/438043a.
117. Piccardo, G.; Tubino, F. Parametric resonance of flexible footbridges under crowd-induced lateral excitation. *J. Sound Vib.* **2008**, *311*, 353–371. https://doi.org/10.1016/j.jsv.2007.09.008.
118. Pizzimenti, A.D.; Ricciardelli, F. Experimental evaluation of the dynamic lateral loading of footbridges by walking pedestrians. In Proceedings of the 6th International Conference on Structural Dynamics (EURODYN 2005), Paris, France, 4–7 September 2005.
119. Ingólfsson, E.T.; Georgakis, C.T.; Ricciardelli, F.; Jönsson, J. Experimental identification of pedestrian-induced lateral forces on footbridges. *J. Sound Vib.* **2011**, *330*, 1265–1284. https://doi.org/10.1016/j.jsv.2010.09.034.
120. Macdonald, J.H.G. Lateral excitation of bridges by balancing pedestrians. *Proc. R. Soc. A—Math. Phys. Eng. Sci.* **2008**, *465*, 1055–1073. https://doi.org/10.1098/rspa.2008.0367.
121. Bocian, M.; MacDonald, J.H.G.; Burn, J.F. Biomechanically inspired modelling of pedestrian-induced forces on laterally oscillating structures. *J. Sound Vib.* **2012**, *331*, 3914–3929. https://doi.org/10.1016/j.jsv.2012.03.023.
122. Carroll, S.P.; Owen, J.S.; Hussein, M.F.M. Crowd-bridge interaction by combining biomechanical and discrete element models. 8th international conference on structural dynamics (EURODYN 2011), Leuven, Belgium, 4–6 July 2011.
123. Racic, V.; Morin, J.B. Data-driven modelling of vertical dynamic excitation of bridges induced by people running. *Mech. Syst. Signal Proc.* **2014**, *43*, 153–170. https://doi.org/10.1016/j.ymssp.2013.10.006.
124. Ellis, B.R.; Ji, T. Loads generated by jumping crowds: Numerical modelling. *Struct. Eng.* **2004**, *82*, 35–40. https://doi.org/10.1109/ICDM.2003.1250957.
125. Xiong, J.; Chen, J.; Caprani, C. Spectral analysis of human-structure interaction during crowd jumping. *Appl. Math. Model.* **2021**, *89*, 610–626. https://doi.org/10.1016/j.apm.2020.07.030.
126. Xiong, J.; Chen, J. Power spectral density function for individual jumping load. *Int. J. Struct. Stab. Dyn.* **2018**, *18*, 1850023. https://doi.org/10.1142/S0219455418500232.
127. Ji, T.; Ellis, B.R. Floor vibration induced by dance-type loads: Theory. *Struct. Eng.* **1994**, *72*, 37–44.
128. Parkhouse, J.G.; Ewins, D.J. Crowd-induced rhythmic loading. *Proc. Inst. Civ. Eng.-Struct. Build.* **2006**, *159*, 247–259. https://doi.org/10.1680/stbu.2006.159.5.247.
129. Duarte, E.; Ji, T. Action of individual bouncing on structures. *J. Struct. Eng.* **2009**, *135*, 818–827. https://doi.org/10.1061/(ASCE)0733-9445(2009)135:7(818).
130. Dougill, J.W.; Wright, J.R.; Parkhouse, J.G.; Harrison, R.E. Human structure interaction during rhythmic bobbing. *Struct. Eng.* **2006**, *84*, 32–39.
131. Wang, H.Q.; Chen, J.; Nagayama, T. Parameter identification of spring-mass-damper model for bouncing people. *J. Sound Vib.* **2019**, *456*, 13–29. https://doi.org/10.1016/j.jsv.2019.05.034.
132. Ahmadi, E.; Caprani, C.; Živanović, S.; Heidarpour, A. Vertical ground reaction forces on rigid and vibrating surfaces for vibration serviceability assessment of structures. *Eng. Struct.* **2018**, *172*, 723–738. https://doi.org/10.1016/j.engstruct.2018.06.059.
133. Kerr, S.C.; Bishop, N.W.M. Human induced loading on flexible staircases. *Eng. Struct.* **2001**, *23*, 37–45. https://doi.org/10.1016/S0141-0296(00)00020-1.
134. Helbing, D.; Buzna, L.; Johansson, A.; Werner, T. Self-organized pedestrian crowd dynamics: Experiments, simulations, and design solutions. *Transp. Sci.* **2005**, *39*, 1–24. https://doi.org/10.1287/trsc.1040.0108.
135. He, W.; Xie, W.; Chen, B.; Sun, L. Assessment on vibration serviceability of large-span railway station under crowd load. In Proceedings of the 5th International Symposium on Environmental Vibration (ISEV2011), Chengdu, China, 20–22 October 2011.
136. Carroll, S.P.; Owen, J.S.; Hussein, M.F.M. Modelling crowd-bridge dynamic interaction with a discretely defined crowd. *J. Sound Vib.* **2012**, *331*, 2685–2709. https://doi.org/10.1016/j.jsv.2012.01.025.
137. Helbing, D.; Molnár, P.; Social force model for pedestrian dynamics. *Phys. Rev. E* **1995**, *51*, 4282–4286. https://doi.org/10.1103/PhysRevE.51.4282.
138. Pu, X.; He, T.; Zhu, Q. Considering the effect of obstacles and semi-rigid boundary conditions on the dynamic response of the floor under random crowd-structure interaction. *Acta Mech.* **2023**, *234*, 3821–3841. https://doi.org/10.1007/s00707-023-03595-2.
139. Xiong, J.; Chen, J. A generative adversarial network model for simulating various types of human-induced loads. *Int. J. Struct. Stab. Dyn.* **2019**, *19*, 1950092. https://doi.org/10.1142/S0219455419500925.
140. Dong, J.K.; Ye, M. Design for random response of structures subject to rhythmic crowd loading. *Buildings* **2023**, *13*, 1085. https://doi.org/10.3390/buildings13041085.
141. Martinelli, L.; Racic, V.; Lago, B.A.D.; Foti, F. Testing walking-induced vibration of floors using smartphones recordings. *Robotics* **2020**, *9*, 37. https://doi.org/10.3390/robotics9020037.
142. Xiong, J.; Cao, Z.; Duan, S.; Cao, B.; Qian, H.; Li, C. A fourier series-based multi-point excitation model for crowd jumping loads. *Buildings* **2023**, *13*, 1782. https://doi.org/10.3390/buildings13071782.
143. Davenport, A.G. The application of statistical concepts to the wind loading of structures. *Proc. Inst. Civ. Eng.* **1961**, *19*, 449–472. https://doi.org/10.1680/iicep.1961.11304.
144. Ruscheweyh, H.; Sedlacek, G. Crosswind vibrations of steel stacks. -critical comparison between some recently proposed codes. *J. Wind Eng. Ind. Aerodyn.* **1988**, *30*, 173–183. https://doi.org/10.1016/0167-6105(88)90082-7.
145. Bishop, R.E.D.; Hassan, A.Y. The lift and drag forces on a circular cylinder oscillating in a flowing fluid. *Proc. R. Soc. Lond. Ser. A—Math. Phys. Sci.* **1964**, *277*, 51–75. https://doi.org/10.1098/rspa.1964.0005.

146. Tamura, Y.; Matsui, G. Wake-oscillator model of vortex-induced oscillation of circular cylinder. In Proceedings of the 5th International Conference, Fort Collins, CO, USA, 8–14 July 1979.
147. Vickery, B.J.; Basu, R.I. Across-wind vibrations of structures of circular cross-section, part i: Development of a mathematical model fort wo-dimensional conditions. *J. Wind Eng. Ind. Aerodyn.* **1983**, *12*, 49–73. https://doi.org/10.1016/0167-6105(83)90080-6.
148. Ehsan, F.; Scanlan, R.H. Vortex-induced vibrations of flexible bridges. *J. Eng. Mech.* **1990**, *116*, 1392–1411. https://doi.org/10.1061/(ASCE)0733-9399(1990)116:6(1392).
149. Larsen, A. A generalized model for assessment of vortex-induced vibration of flexible structures. *J. Wind Eng. Ind. Aerodyn.* **1995**, *57*, 281–294. https://doi.org/10.1016/0167-6105(95)00008-F.
150. Wijesooriya, K.; Mohotti, D.; Amin, A.; Chauhan, K. An uncoupled fluid structure interaction method in the assessment of structural responses of tall buildings. *Structures* **2020**, *25*, 448–462. https://doi.org/10.1016/j.istruc.2020.03.031.
151. Li, Y.; Zhu, Y.; Chen, F.; Li, Q.S. Aerodynamic loads of tapered tall buildings: Insights from wind tunnel test and CFD. *Structures* **2023**, *56*, 104975. https://doi.org/10.1016/j.istruc.2023.104975.
152. Simiu, E.; Yeo, D. *Wind Effects on Structures: Modern Structural Design for Wind*; John Wiley & Sons, Inc.: Hoboken, NJ, USA, 2019.
153. *JGJ 3-2010*; Technical Specification for Concrete Structures of Tall Building. Ministry of Housing and Urban-Rural Development: Beijing, China, 2010.
154. *JGJ 99-2015*; Technical Specification for Steel Structure of Tall Building. Ministry of Housing and Urban-Rural Development: Beijing, China, 2015.
155. *AIJ-GEH-2004*; Guidelines for the Evaluation of Habitability to Building Vibration. Architectural Institute of Japan: Tokyo, Japan, 2007.
156. *ISO 6897-1984*; Guidelines for the Evaluation of the Response of Occupants of Fixed Structures, Especially Buildings and Offshore Structures, to Low-frequency Horizontal Motion (0.063 to 1Hz). International Standard Organization: Geneva, Switzerland, 1984.
157. Hu, W.; Teng, D.; Li, J.; Xu, Z.; Wang, Y.; Lu, W.; Li, Z.; Teng, J. Structural Dynamic Parameter Identification of Saige Building Based on Distributed Synchronous Acquisition Method. *J. Build. Struct.* **2022**, *43*, 76–84. https://doi.org/10.14006/j.jzjgxb.2022.0050.
158. Xu, W.; Li, R.; Qiu, J.; Li, Q.; Yu, Z. Study on wind-induced human comfort of the SEG plaza under local excitation based on wind tunnel test. *Sustainability* **2023**, *15*, 3067. https://doi.org/10.3390/su15043067.
159. Zhou, H.; Shao, X.; Zhang, J.; Yao, H.; Liu, Y.; Tan, P.; Chen, Y.; Xu, L.; Zhang, Y.; Gong, W. Real-time hybrid model test to replicate high-rise building resonant vibration under wind loads. *Thin-Walled Struct.* **2024**, *197*, 111559. https://doi.org/10.1016/j.tws.2024.111559.
160. Yang, Y.; Ma, F.; Han, Q. Reconstruction of boundary layer wind field at the seg plaza based on dual-lidar measurement and numerical simulation. *J. Wind Eng. Ind. Aerodyn.* **2023**, *223*, 105298. https://doi.org/10.1016/j.jweia.2023.105298.
161. Xie, W.; Zhu, M.; Yin, Y.; Tang, Z.; Peng, Q.; Cheng, Y. Research on vibration and secondary noise induced by elevator car-guiderail coupling. *Noise Vib. Control* **2023**, *43*, 74–81. https://doi.org/10.3969/j.issn.1006-1355.2023.04.012.
162. Zhang, X.; Wang, Y.; Xie, W. Research on structure vibration and secondary noise caused by 220 kV transformers. *Noise Vib. Control* **2020**, *40*, 188–193. https://doi.org/10.3969/j.issn.1006-1355.2020.03.033.
163. Li, H.; Yang, W.; Liu, P.; Wang, M. Resonance measurement and vibration reduction analysis of an office building induced by nearby crane workshop vibration. *J. Build. Eng.* **2022**, *58*, 105018. https://doi.org/10.1016/j.jobe.2022.105018.
164. Hwang, J.H.; Tu, T.Y. Ground vibration due to dynamic compaction. *Soil Dyn. Earthq. Eng.* **2006**, *26*, 337–346. https://doi.org/10.1016/j.soildyn.2005.12.004.
165. Valeria, L.; Annamaria, L.; Gaetano, E.; Domenico, R.; Giuseppina, U. Vibrations induced by mechanical rock excavation on R.C. buildings in an urban area. *Buildings* **2021**, *11*, 15. https://doi.org/10.3390/buildings11010015.
166. *ISO 2631-1:1997*; Mechanical Vibration and Shock—Evaluation of Human Exposure to Whole Body Vibration Part 1: General Requirements. International Organization for Standardization: Geneva, Switzerland, 1997.
167. *ISO 2631-1:1997/Amd 1:2010*; Mechanical Vibration and Shock—Evaluation of Human Exposure to Whole-body Vibration—Part 1: General Requirements Amendment 1. International Organization for Standardization: Geneva, Switzerland, 2010.
168. He, W.; Xie, W. Study on sophisticated calculation model of large-span railway station structures based on vibration serviceability evaluation. *China Civ. Eng. J.* **2014**, *47*, 13–23. https://doi.org/10.15951/j.tmgcxb.2014.01.005.
169. Zhu, Q.; Liu, K.; Liu, L.; Du, Y.; Zivanovic, S. Experimental and numerical analysis on serviceability of cantilevered floor based on human-structure interaction. *J. Constr. Steel. Res.* **2020**, *173*, 106184. https://doi.org/10.1016/j.jcsr.2020.106184.
170. Xie, Z.; Hu, X.; Du, H.; Zhang, X. Vibration behavior of timber-concrete composite floors under human-induced excitation. *J. Build. Eng.* **2020**, *32*, 101744. https://doi.org/10.1016/j.jobe.2020.101744.
171. Xue, S.; Zhang, Z.; Zhang, Z.; Zhou, H.; Shen, Y. Effects of strongbacks and strappings on vibrations of timber truss joist floors. *Shock Vib.* **2021**, *2021*, 6630719. https://doi.org/10.1155/2021/6630719.
172. An, Q.; Ren, Q.; Liu, H.; Yan, X.; Chen, Z. Dynamic performance characteristics of an innovative cable supported beam structure—Concrete slab composite floor system under human-induced loads. *Eng. Struct.* **2016**, *117*, 40–57. https://doi.org/10.1016/j.engstruct.2016.02.038.
173. Astroza, R.; Ebrahimian, H.; Conte, J.P.; Restrepo, J.I.; Hutchinson, T.C. Influence of the construction process and nonstructural components on the modal properties of a five-story building. *Earthq. Eng. Struct. Dyn.* **2016**, *45*, 1063–1084. https://doi.org/10.1002/eqe.2695.

174. Devin, A.; Fanning, P.J. Non-structural elements and the dynamic response of buildings: A review. *Eng. Struct.* **2019**, *187*, 242–250. https://doi.org/10.1016/j.engstruct.2019.02.044.
175. Liang, H.; Xie, W.; Wei, P.; Zhou, Y.; Zhang, Z. The effect of the decorative surface layer on the dynamic properties of a symmetric concrete slab. *Symmetry* **2021**, *13*, 1174. https://doi.org/10.3390/sym13071174.
176. Reynolds, P.; Pavic, A. Effects of false floors on vibration serviceability of building floors. I: Modal properties. *J. Perform. Constr. Facil.* **2003**, *17*, 75–86. https://doi.org/10.1061/(ASCE)0887-3828(2003)17:2(75).
177. Jiménez-Alonso, J.F.; Pérez-Aracil, J.; Díaz, H.A.M.; Sáez, A. Effect of vinyl flooring on the modal properties of a steel footbridge. *Appl. Sci.* **2019**, *9*, 1374. https://doi.org/10.3390/app9071374.
178. Miskovic, Z.; Pavic, A.; Reynolds, P. Effects of full-height nonstructural partitions on modal properties of two nominally identical building floors. *Can. J. Civ. Eng.* **2009**, *36*, 1121–1132. https://doi.org/10.1139/L09-055.
179. Li, B.; Hutchinson, G.L.; Duffield, C.F. The influence of non-structural components on tall building stiffness. *Struct. Des. Tall Spec. Build.* **2011**, *20*, 853–870. https://doi.org/10.1002/tal.565.
180. Wang, Z.; Song, L.; Cheng, Z.; Yang, H.; Wen, J.; Qi, M. Finite element model for vibration serviceability evaluation of a suspended floor with and without tuned mass dampers. *Buildings* **2023**, *13*, 309. https://doi.org/10.3390/buildings13020309.
181. Pedersen, L.H.; Frier, C.; Andersen, L. Flooring-systems and Their Interaction with Usage of the Floor. In *Dynamics of Civil Structures*; Caicedo, J., Pakzad, S., Eds.; The Society for Experimental Mechanics, Inc.: Danbury, CT, USA, 2017; pp. 205–211.
182. Setareh, M. Vibration serviceability of a building floor structure. I: Dynamic testing and computer modeling. *J. Perform. Constr. Facil.* **2010**, *24*, 497–507. https://doi.org/10.1061/(ASCE)CF.1943-5509.0000134.
183. Huang, M.; Ling, Z.; Sun, C.; Lei, Y.; Xiang, C.; Wan, Z.; Gu, J. Two-stage damage identification for bridge bearings based on sailfish optimization and element relative modal strain energy. *Struct. Eng. Mech.* **2023**, *86*, 715–730. https://doi.org/10.12989/sem.2023.86.6.715.
184. Gidrão, G.d.M.S.; Carrazedo, R.; Bosse, R.M.; Silvestro, L.; Ribeiro, R.; Souza, C.F.P.d. Numerical modeling of the dynamic elastic modulus of concrete. *Materials* **2023**, *16*, 3955. https://doi.org/10.3390/ma16113955.
185. Amabili, M. Nonlinear damping in large-amplitude vibrations: Modelling and experiments. *Nonlinear Dyn.* **2018**, *93*, 5–18. https://doi.org/10.1007/s11071-017-3889-z.
186. He, Y.; Liu, Y.; Wu, M.; Fu, J.; He, Y. Amplitude dependence of natural frequency and damping ratio for 5 supertall buildings with moderate-to-strong typhoon-induced vibrations. *J. Build. Struct.* **2023**, *78*, 107589. https://doi.org/10.1016/j.jobe.2023.107589.
187. Han, Z.; Brownjohn, J.M.W.; Chen, J. Structural modal testing using a human actuator. *Eng. Struct.* **2020**, *221*, 111113. https://doi.org/10.1016/j.engstruct.2020.111113.
188. Onundi, L.O.; Elinwa, A.U.; Matawal, D.S. An experimental determination of damping ratio of a multi-storey building subjected to aerodynamic loadings. *J. Civ. Eng. Constr. Technol.* **2012**, *3*, 127–139. https://doi.org/10.5897/JCECT11.063.
189. Luo, J.; Huang, M.; Lei, Y. Temperature effect on vibration properties and vibration-based damage identification of bridge structures: A literature review. *Buildings* **2022**, *12*, 1209. https://doi.org/10.3390/buildings12081209.
190. Wang, Z.; Huang, M.; Gu, J. Temperature effects on vibration-based damage detection of a reinforced concrete slab. *Appl. Sci.* **2020**, *10*, 2869. https://doi.org/10.3390/app10082869.
191. *ISO 2631-2:2003*; Mechanical Vibration and Shock—Evaluation of Human Exposure to Wholebody Vibration—Part 2: Vibration in Buildings (1 Hz to 80 Hz). International Organization for Standardization: Geneva, Switzerland, 2003.
192. *GB 10070-88*; Standard of Environmental Vibration in Urban Area. Ministry of Ecology and Environment: Beijing, China, 1988.
193. *JGJ/T 170-2009*; Standard for Limit and Measuring Method of Building Vibration and Secondary Noise Caused by Urban Rail Transit. Ministry of Housing and Urban-Rural Development: Beijing, China, 2009.
194. Applied Technology Council. *ATC Design Guide 1, Minimizing Floor Vibration*; Applied Technology Council: Redwood City, CA, USA, 1999.
195. AISC. *AISC Design Guide 11, Floor Vibrations Due to Human Activity*; American Institute of Steel Construction: Chicago, IL, USA, 2001.
196. *EN 1990: 2002*; Eurocode—Basis of Structural Design. British Standards Institution: London, UK, 2002.
197. *BS 6472-1: 2008*; Guide to Evaluation of Human Exposure to Vibration in Buildings. British Standards Institution: London, UK, 2008.
198. *AIJ ES-V001-2018*; Guidelines for the Evaluation of Habitability to Building Vibration. Architectural Institute of Japan: Tokyo, Japan, 2018.
199. Xiong, J.; Liu, Z.; Duan, S.; Qian, H. A review of evaluation methods of standards for structural vibration serviceability under crowd walking. *Buildings* **2024**, *14*, 675. https://doi.org/10.3390/buildings14030675.
200. *ISO 2631/1-1985*; Evaluation of Human Exposure to Whole-body Vibration—Part 1: General Requirements. International Organization for Standardization: Geneva, Switzerland, 1985.
201. Tao, Z.; Wang, Y.; Sanayei, M.; Moore, J.A.; Zou, C. Experimental study of train-induced vibration in over-track buildings in a metro depot. *Eng. Sturct.* **2019**, *198*, 109473. https://doi.org/10.1016/j.engstruct.2019.109473.
202. Farahani, M.V.; Sadeghi, J.; Jahromi, S.G.; Sahebi, M.M. Modal based method to predict subway train-induced vibration in buildings. *Structures* **2023**, *47*, 557–572. https://doi.org/10.1016/j.istruc.2022.11.092.
203. Hua, Y.; Xie, W.; Chen, B. Research on influence of metro vibration on vertical floor response of buildings. *J. Build. Struct.* **2023**, *44*, 122–129. https://doi.org/10.14006/j.jzjgxb.2020.0520.

204. Xia, H.; Zhang, N.; Cao, Y. Experimental study of train-induced vibrations of environments and buildings. *J. Sound Vib.* **2005**, *280*, 1017–1029. https://doi.org/10.1016/j.jsv.2004.01.006.
205. Xia, H.; Chen, J.; Wei, P.; Xia, C.; Roeck, G.D.; Degrande, G. Experimental investigation of railway train-induced vibrations of surrounding ground and a nearby multi-story building. *Earthq. Eng. Eng. Vib.* **2009**, *8*, 137–148. https://doi.org/10.1007/s11803-009-8101-0.
206. Xia, Q.; Qu, W. Experimental and numerical studies of metro train-induced vibrations on adjacent masonry buildings. *Int. J. Struct. Stab. Dyn.* **2016**, *16*, 1550067. https://doi.org/10.1142/S0219455415500674.
207. Yu, Y.; Xie, W.; Song, B. The vibration measurement and evaluation due to the traffic loads. In *Proceedings of the International Seminar on Environmental Vibration: Prediction, Monitoring and Evaluation*; China Communications Press: Hangzhou, China, 2003.
208. Du, H.; Du, S.; Li, W. Probabilistic time series forecasting with deep non-linear state space models. *CAAI T. Intell. Technol.* **2023**, *8*, 3–13. https://doi.org/10.1049/cit2.12085.
209. Wan, S.; Guan, S.; Tang, Y. Advancing bridge structural health monitoring: Insights into knowledge-driven and data-driven approaches. *J. Data Sci. Intell. Syst.* **2023**, *00*, 1–12. https://doi.org/10.47852/bonviewJDSIS3202964.
210. Wang, W.; Sun, Y.; Li, K.; Wang, J.; He, C.; Sun, D. Fully bayesian analysis of the relevance vector machine classification for imbalanced data problem. *CAAI T. Intell. Technol.* **2023**, *8*, 192–205. https://doi.org/10.1049/cit2.12111.
211. Chen, D.; Wu, J.; Yan, Q. A novel smartphone-based evaluation system of pedestrian-induced footbridge vibration comfort. *Adv. Struct. Eng.* **2019**, *22*, 1685–1697. https://doi.org/10.1177/1369433218824906.
212. Cao, L.; Chen, J. Online investigation of vibration serviceability limitations using smartphones. *Measurement* **2020**, *162*, 107850. https://doi.org/10.1016/j.measurement.2020.107850.
213. Deng, Z.; Huang, M.; Wan, N.; Zhang, J. The current development of structural health monitoring for bridges: A review. *Buildings* **2023**, *13*, 1360. https://doi.org/10.3390/buildings13061360.
214. Zhang, J.; Huang, M.; Wan, N.; Deng, Z.; He, Z.; Luo, J. Missing measurement data recovery methods in structural health monitoring: The state, challenges and case study. *Measurement* **2024**, *231*, 114528. https://doi.org/10.1016/j.measurement.2024.114528.
215. Sol-Sánchez, M.; Moreno-Navarro, F.; Rubio-Gámez, M.C. The use of elastic elements in railway tracks: A state of the art review. *Constr. Build. Mater.* **2015**, *75*, 293–305. https://doi.org/10.1016/j.conbuildmat.2014.11.027.
216. Ouakka, S.; Verlinden, O.; Kouroussis, G. Railway ground vibration and mitigation measures: Benchmarking of best practice. *Railw. Eng. Sci.* **2022**, *30*, 1–22. https://doi.org/10.1007/s40534-021-00264-9.
217. Wang, Y.; He, Z.; Wang, K.; Bai, Y.; Li, P. Comparing dynamic performance between new sleeper-damping and floating-slab track system. *Constr. Build. Mater.* **2023**, *400*, 132588. https://doi.org/10.1016/j.conbuildmat.2023.132588.
218. Hu, Y.; Cheng, Z.; Shi, Z. Vibration reduction performance of a periodic layered slab track. *Adv. Environ. Vib. Transp. Geeodyn.* **2020**, *66*, 779–791. https://doi.org/10.1007/978-981-15-2349-6_50.
219. Sung, D.; Chang, S.; Kim, S. Effect of additional anti-vibration sleeper track considering sleeper spacing and track support stiffness on reducing low-frequency vibrations. *Constr. Build. Mater.* **2020**, *263*, 120140. https://doi.org/10.1016/j.conbuildmat.2020.120140.
220. Qu, S.; Ding, W.; Dong, L.; Zhu, J.; Zhu, S.; Yang, Y.; Zhai, W. Chiral phononic crystal-inspired railway track for low-frequency vibration suppression. *Int. J. Mech. Sci.* **2024**, *274*, 109275. https://doi.org/10.1016/j.ijmecsci.2024.109275.
221. Mahdavisefat, E.; Heshmati, A.; Salehzadeh, H.; Bahmani, H.; Sabermahani, M.; Vibration screening by trench barriers, a review. *Arab. J. Geosci.* **2017**, *10*, 513. https://doi.org/10.1007/s12517-017-3279-3.
222. Meng, L.; Shi, Z.; Hao, S.; Cheng, Z. Filtering property of periodic in-filled trench barrier for underground moving loads. *Constr. Build. Mater.* **2023**, *400*, 132655. https://doi.org/10.1016/j.conbuildmat.2023.132655.
223. Yao, J.; Zhao, R.; Zhang, N.; Yang, D. Vibration isolation effect study of in-filled trench barriers to train-induced environmental vibrations. *Soil Dyn. Earthq. Eng.* **2019**, *125*, 105741. https://doi.org/10.1016/j.soildyn.2019.105741.
224. Ai, Z.Y.; Cao, Z. Vibration isolation of row of piles embedded in transverse isotropic multi-layered soils. *Comput. Geotech.* **2018**, *99*, 115–129. https://doi.org/10.1016/j.compgeo.2018.03.002.
225. Takemiya, H. Field vibration mitigation by honeycomb WIB for pile foundations of a high-speed train viaduct. *Soil Dyn. Earthq. Eng.* **2003**, *24*, 69–87. https://doi.org/10.1016/j.soildyn.2003.07.005.
226. Cao, X.; Zhou, F.; Liu, J.; Ma, Q. Experimental study and numerical analysis for vibration isolation performance on open trench and wave impeding block combined vibration isolation barrier. *Soil Dyn. Earthq. Eng.* **2024**, *177*, 108418. https://doi.org/10.1016/j.soildyn.2023.108418.
227. Chen, J.; Geng, J.; Gao, G.; Luo, W.; Liu, Y.; Li, K. Mitigation of subway-induced low-frequency vibrations using a wave impeding block. *Transp. Geotech.* **2022**, *37*, 100862. https://doi.org/10.1016/j.trgeo.2022.100862.
228. Pu, X.; Shi, Z. Broadband surface wave attenuation in periodic trench barriers. *J. Sound Vib.* **2020**, *468*, 115130. https://doi.org/10.1016/j.jsv.2019.115130.
229. James, P. Base-isolated buildings: Towards performance based design. *Proc. Inst. Civ. Eng.-Struct. Build.* **2016**, *169*, 574–582. https://doi.org/10.1680/jstbu.15.00057.
230. Pan, P.; Shen, S.; Shen, Z.; Gong, R. Experimental investigation on the effectiveness of laminated rubber bearings to isolate metro generated vibration. *Measurement* **2018**, *122*, 554–562. https://doi.org/10.1016/j.measurement.2017.07.019.
231. Liang, Q.; Zhou, Y.; Wang, D.; Luo, W.; Li, J.; He, Z. Shaking table test of vertical isolation performances of super high-rise structure under metro train-induced vibration. *J. Build. Eng.* **2024**, *82*, 108323. https://doi.org/10.1016/j.jobe.2023.108323.

232. *T/CECS 1234-2023*; Technical Standard for Integrated Control of Engineering Vibration and Seismic Vibration of Building Engineering: China Association for Engineering Construction Standardization, Beijing, China, 2023.
233. Cao, Y.R.; Pan, P.; Sun, J.B.; Wang, H.S. Mechanical properties and isolation effect of disc spring-single friction pendulum 3D vibration isolation device. *J. Build. Struct.* **2022**, *43*, 44–53. https://doi.org/10.14006/j.jzjgxb.2020.0721.
234. Cao, Y.; Pan, P.; Wang, H.; Sun, J.; Xiao, G.; Zuo, Z. Development of an innovative three-dimensional vibration isolation bearing. *Eng. Struct.* **2023**, *295*, 116890. https://doi.org/10.1016/j.engstruct.2023.116890.
235. Sheng, T.; Liu, G.; Bian, X.; Shi, W.; Chen, Y. Development of a three-directional vibration isolator for buildings subject to metro- and earthquake-induced vibrations. *Eng. Struct.* **2022**, *252*, 113576. https://doi.org/10.1016/j.engstruct.2021.113576.
236. Liang, Q.; Luo, W.; Zhou, Y.; Lu, Z.; Li, J.; He, Z. Vibration filtering effect of a novel three-dimensional isolation bearing on metro vibration isolation. *Eng. Struct.* **2024**, *301*, 117304. https://doi.org/10.1016/j.engstruct.2023.117304.
237. He, W.; Luo, H.; Chang, W.; Xu, H.; Liu, W.; Zhang, Q. Experiment investigation and in situ test of hybrid vibration bearing system applied to overtrack historical buildings. *Struct. Control Health Monit.* **2022**, *29*, e2921. https://doi.org/10.1002/stc.2921.
238. Rahimi, F.; Aghayari, R.; Samali, B. Application of tuned mass dampers for structural vibration control: A state-of-the-art review. *Civ. Eng. J.* **2020**, *6*, 1622–1651. https://doi.org/10.28991/cej-2020-03091571.
239. Elias, S.; Matsagar, V. Research developments in vibration control of structures using passive tuned mass dampers. *Annu. Rev. Control* **2017**, *44*, 129–156. https://doi.org/10.1016/j.arcontrol.2017.09.015.
240. Wang, Z.; Chen, Y.; Hu, M.; Chen, A. Vertical vibration and TMD mitigation of an industrial building floor subjected to machine excitation. *J. Vib. Eng.* **2019**, *32*, 986–995. https://doi.org/10.16385/j.cnki.issn.1004-4523.2019.06.007.
241. Elias, S.; Matsagar, V. Distributed multiple tuned mass dampers for wind vibration response control of high-rise building. *J. Eng.* **2014**, *2014*, 198719. https://doi.org/10.1155/2014/198719.
242. Li, C.; Pan, H.; Cao, L. Pendulum-type tuned tandem mass dampers-inerters for crosswind response control of super-tall buildings. *J. Wind Eng. Ind. Aerodyn.* **2024**, *247*, 105706. https://doi.org/10.1016/j.jweia.2024.105706.
243. Cao, H.Q. Combined tuned mass dampers for structural vibration control. *Int. J. Non-Linear Mech.* **2023**, *157*, 104550. https://doi.org/10.1016/j.ijnonlinmec.2023.104550.
244. Roozbahan, M.; Turan, G. An improved passive tuned mass damper assisted by dual stiffness. *Structures* **2023**, *50*, 1598–1607. https://doi.org/10.1016/j.istruc.2023.02.125.
245. Li, Y.; Tan, P.; Li, S.; He, H. A novel tuned inerter eddy current damper: Modeling, optimization, and evaluation. *Eng. Struct.* **2023**, *285*, 116026. https://doi.org/10.1016/j.engstruct.2023.116026.
246. Wang, L.; Nagarajaiah, S.; Shi, W.; Zhou, Y. Semi-active control of walking-induced vibrations in bridges using adaptive tuned mass damper considering human-structure-interaction. *Eng. Struct.* **2021**, *244*, 112743. https://doi.org/10.1016/j.engstruct.2021.112743.
247. Wang, L.; Zhou, Y.; Shi, W. Random crowd-induced vibration in footbridge and adaptive control using semi-active TMD including crowd-structure interaction. *Eng. Struct.* **2024**, *306*, 117839. https://doi.org/10.1016/j.engstruct.2024.117839.
248. Zhang, C.W. The active rotary inertia driver system for flutter vibration control of bridges and various promising applications. *Sci China Tech. Sci.* **2023**, *66*, 390–405. https://doi.org/10.1007/s11431-022-2228-0.
249. Kang, X.; Huang, Q.; Wu, Z.; Tang, J.; Jiang, X.; Lei, S. A review of the tuned mass damper inerter (TMDI) in energy harvesting and vibration control: Designs, analysis and applications. *Comp. Model. Eng. Sci.* **2024**, *139*, 2361–2398. https://doi.org/10.32604/cmes.2023.043936.
250. Ikeda, K.; Ioi, T. On the dynamic vibration damped absorber of the vibration system. *Trans. Jpn. Soc. Mech. Eng.* **1977**, *43*, 1707–1715. https://doi.org/10.1299/kikai1938.43.1707.
251. Liu, Y.; Lin, C.C.; Parker, J.; Zuo, L. Exact H_2 optimal tuning and experimental verification of energy-harvesting series electromagnetic tuned-mass dampers. *J. Vib. Acoust.* **2016**, *138*, 061003. https://doi.org/10.1115/1.4034081.
252. Kamariotis, A.; Chatzi, E.; Straub, D. A framework for quantifying the value of vibration-based structural health monitoring. *Mech. Syst. Signal Proc.* **2023**, *184*, 109708. https://doi.org/10.1016/j.ymssp.2022.109708.
253. Alarcon, M.; Soto, P.; Hernandez, F.; Guindos, P. Structural health monitoring of South America's first 6-story experimental light-frame timber-building by using a low-cost RaspberryShake seismic instrumentation. *Eng. Struct.* **2023**, *275*, 115278. https://doi.org/10.1016/j.engstruct.2022.115278.